ACS MEASUREMENT SCIENCE Au
AN OPEN ACCESS JOURNAL OF THE AMERICAN CHEMICAL SOCIETY

pubs.acs.org/measureau
Perspective

Nanoscale Luminescence Imaging/Detection of Single Particles: State-of-the-Art and Future Prospects

Published as part of ACS Measurement Science Au virtual special issue "2023 Rising Stars".

Muhammad Saqib,* Mariam Zafar, Mohamed Ibrahim Halawa, Shahzad Murtaza, Ghulam Mustafa Kamal, and Guobao Xu

Cite This: *ACS Meas. Sci. Au* 2024, 4, 3−24

Read Online

ACCESS | Metrics & More | Article Recommendations

ABSTRACT: Single-particle-level measurements, during the reaction, avoid averaging effects that are inherent limitations of conventional ensemble strategies. It allows revealing structure−activity relationships beyond averaged properties by considering crucial particle-selective descriptors including structure/morphology dynamics, intrinsic heterogeneity, and dynamic fluctuations in reactivity (kinetics, mechanisms). In recent years, numerous luminescence (optical) techniques such as chemiluminescence (CL), electrochemiluminescence (ECL), and fluorescence (FL) microscopies have been emerging as dominant tools to achieve such measurements, owing to their diversified spectroscopy principles, noninvasive nature, higher sensitivity, and sufficient spatiotemporal resolution. Correspondingly, state-of-the-art methodologies and tools are being used for probing (real-time, operando, in situ) diverse applications of single particles in sensing, medicine, and catalysis. Herein, we provide a concise and comprehensive perspective on luminescence-based detection and imaging of single particles by putting special emphasis on their basic principles, mechanistic pathways, advances, challenges, and key applications. This Perspective focuses on the development of emission intensities and imaging based individual particle detection. Moreover, several key examples in the areas of sensing, motion, catalysis, energy, materials, and emerging trends in related areas are documented. We finally conclude with the opportunities and remaining challenges to stimulate further developments in this field.

KEYWORDS: *Single-particles, luminescence, imaging, operando, structure−activity relationship*

1. INTRODUCTION

Single-entity imaging and detection is a rapid-progressing field. The concept describes a recent trend for studying an individual "process or entity" at a time that can be a reaction, a cell, a molecule, or a nanoparticle (NP).[1] For the particles, each of them has distinct surface chemistry, lattice defects, atomic arrangement, morphology, and chemical composition, which results in considerably different activities during chemical and electrochemical processes.[2] Ensemble recordings only measure the average response of various particles, which denies access to the microscopic picture at a single entity level.[3,4] Therefore, single particle detection is an overarching measurement concept that is driven by a desire to understand heterogeneity (both spatially and among population), recording of faster processes, exploring the underlying mechanisms, optimizing the reactions performance/ yields/ outcomes, improvement of analytical detection, and addressing emerging questions from inherently interdisciplinary fields including catalysis and surface science,[5,6] cellular biology,[7] drug delivery, and so on.[8,9]

Traditionally, reaction mechanisms, performance, kinetics, and chemical (photochemical, electrochemical, photoelectrochemical) properties are optimized and measured at the bulk level, wherein chemical systems are composed of ensemble/ larger collection of particles.[10] Such recordings can only provide averaged (entire ensembles) quantities and presents general trends and insights about chemical reactivities of particles.[2] However, the precise/ accurate information about the reactivity of single particles will be lost in the average-ensemble measurements because single particles behave differently (heterogeneously) in catalytic processes, on surfaces, or in complex media.[2,11] Chemical measurements on the level of an individual particle, individual molecule, or individual site eliminate or reduce the loss of valuable information. Therefore, measuring the single particle response is essential to uncover

Received: September 14, 2023
Revised: October 28, 2023
Accepted: November 13, 2023
Published: December 7, 2023

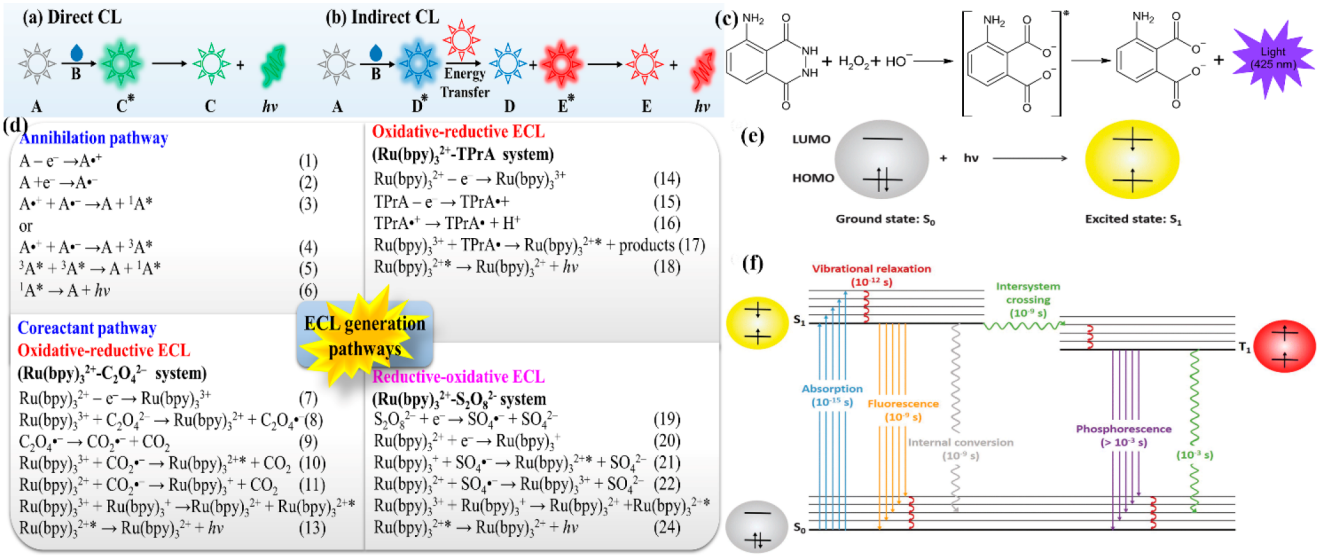

Figure 1. Schematic representation of direct (a) and indirect (b) CL. Asterisk (*) indicates the excited product. (c) Schematic showing the CL generation mechanism of a classical luminol-H_2O_2 system with a blue emission at 425 nm. (d) Schematic showing typical examples of annihilation and coreactant pathways for ECL generation. Asterisk (*) indicates the excited product. (e) Schematic illustration of the molecular orbital for demonstrating the general principle of PL. (f) Jablonski diagram displaying the typical photophysical processes in molecule. Reprinted from ref 61 with permission from the Royal Society of Chemistry, copyright 2019.

their intrinsic heterogeneities, particle specific properties, structure−activity correlations, and mechanistic pathways.

Nanoscale measurement of single particles requires both sufficient signal-to-noise ratio (SNR) and separation of the one particle response to achieve target detection.[12] To achieve these targets, traditional chemical techniques alone cannot offer sufficient information to fully explore the electrochemical systems because of their limited spatial resolution and lack of molecular information.[13,14] Although conventional electrochemical techniques have been successfully applied for revealing dynamic information and kinetics of electrochemical reaction with enhanced sensitivity.[15,16] However, those techniques are performed on ensembles, which describe the average response (potential, current) of thousands to billions of particles or entire electrode.[17] Therefore, it is crucial to develop powerful platforms (methods) for probing single particle, single site, or single molecule level (electro)chemical processes with nanometer-scale-resolution.

Recently, luminescence (optical) approaches are emerging as powerful single particle imaging/detection tools due to their excellent sensitivity, noninvasive nature, sufficient spatiotemporal resolution, and diversified spectroscopic principles.[2,18] In particular, coupling optical tools with super-resolution chemical measurements currently offer the most useful toolkit for single particle detection/imaging.[19−22] The conversion of the chemical process (input) into optical readout could significantly promote the dynamic range and sensitivity of the imaging/detection methods. Chemiluminescence (CL), electrochemiluminescence (ECL, only applicable to electrochemical process), and fluorescence (FL) are spectacular light generating processes induced by chemical, electrochemical, and photochemical reactions, respectively.[23,24] With combined merits of optical readout and (electro)chemical methods, luminescence approaches show numerous notable superiorities over various other transduction techniques.[25−27] As superior analytical techniques, these approaches possess a broad range of applications in diverse fields.[28−31] Although electrochemical methods (e.g., amperometry) are powerful techniques for reveling the redox events of single nanoparticles with low detection limits and higher temporal resolution.[32,33] However, we mainly focused on luminescence-based techniques coupled with electrochemical methods in this Perspective.

With the advent of microscopies, luminescence based single particle imaging/detection is an emerging area of research.[34−36] It can be broadly categorized into intensity and imaging-based single particle detection.[37,38] These microscopic techniques hold potential advantages in terms of low reagent consumption, high throughput, and good spatiotemporal resolution, which significantly promotes their imaging based single particle detection applications.[27,39] The CL/ECL microscopes show no local photothermal effect (no extrinsic illumination source) and near-zero or low background.[34,40] However, the major obstacle is the weak CL/ECL emission (limited photons) of single particles.[26,41] The development of both CL/ECL microscopic approaches is slow in comparison to that of fluorescence microscopy (FLM).[42]

FLM offers various unique superiorities for real-time probing the nanoscale interfaces with both higher detection (single molecule/particle) sensitivity and higher temporal resolution.[43] In particular, FLM is uniquely suited to probe chemical interfaces for a diverse range of applications such as imaging catalytic heterogeneities, studying electron-transfer kinetics and interfacial nanobubble generation, tracking motion, and constructing multiplex immunoassays at a single particle/molecule level.[44,45] In addition, coupled with new detection strategies and electrode designs, the temporal and spatial resolutions can be achieved up to millisecond and nanometer levels, respectively.[27,46] Single photons could be detected by applying scientific complementary metal-oxide-semiconductor (sCMOS) and electron multiplying charge-coupled device (EMCCD) camera devices.[47] As a result, single particle imaging/detection with high spatial resolution and throughput using these luminescence microscopies has been realized under ambient conditions.[48]

As luminescence based single particle imaging/detection is a rapidly advancing research area, a perspective can promote

https://doi.org/10.1021/acsmeasuresciau.3c00052
ACS Meas. Sci. Au 2024, 4, 3−24

related research by stimulating the generation of novel research questions. As far as we know, a comprehensive/critical perspective on diversified luminescence (CL, ECL, and FL) microscopies for detecting/imaging diverse aspects of dynamic (electro)chemical reactions taking place on certain single particle (nanoscale-level) surfaces is still missing. In this Perspective, we aim to discuss and summarize the mechanistic pathways, fundamental instrumentations/setups, and innovative developments in diverse applications of luminescence-based techniques, especially related to single particle imaging/detection. We also tabulated a brief comparison between these techniques. Finally, we discuss potential challenges and directions for future development in this emerging area of research.

2. MECHANISTIC PATHWAYS

2.1. Light Generation Pathway in CL

In general, three conditions must be met for the successful generation of CL. First, sufficient energy must be generated during a reaction to promote the formation of an electronically excited intermediate or product to happen. Second, an appropriate reaction pathway should necessarily exist to enable this energy to generate an excited state electronically.[49] Third, the electronically excited state product must relax to the ground state either itself resulting in emission of a photon (direct CL; Figure 1a) or transfer its energy to an energy (fluorescent) acceptor (indirect CL; Figure 1b).[29] Until recently, typical CL systems such as acyl hydrazides, acridinium esters, peroxalate derivatives, potassium permanganate, dioxetane derivatives, and tris(2,2-bipyridine)ruthenium(II) ($Ru(bpy)_3^{2+}$) have been extensively utilized for diverse analytical applications.[29,50−52] Almost all such reactions resulted in an oxidative process on the basis of hydrogen peroxide (H_2O_2), oxygen (O_2), or other oxidants.[53,54]

Oxidation of luminol in the presence of H_2O_2 and a catalyst is one of the most widely studied and well-known CL reactions.[55] The direct mechanism of luminol reaction occurs either in the presence of an oxidizing agent or oxygen in basic solution that promote the formation of an excited state of α-hydroxyperoxide, which results in CL emission after coming back to ground state (Figure 1c).[56,57] The CL spectrum of luminol shows a maximum emission at ∼425 nm wavelength in aqueous media which is like the 3-aminophthalate FL spectrum, i.e., the emitting species.[58] The CL emission of luminol can be tuned with the help of structural modifications or chemical enhancers, such as nanomaterials or fluorescent compounds, which can also be utilized to enhance the CL emission of luminol system.[59,60]

2.2. Light Generation Pathway in ECL

The ECL process involves in situ production of the excited state species at the electrode surface, induced by high energy electron transfer reactions. In ECL, the light generation process is induced and controlled by sweeping or switching the electrode potentials. ECL is produced through two dominant pathways: one is called the annihilation pathway, and the second is known as the coreactant pathway.[25]

The initial ECL research was dominantly focused on ion annihilation pathways, while modern ECL analytical applications are mostly centered on coreactant pathways.[62,63] Additionally, ECL can also be generated by electrostatic CL and hot electron-induced pathways.[64]

2.2.1. Annihilation Pathway. In the case of the ion annihilation route, oxidized and reduced species are generated on the surface of the electrode with the help of a sweep or potential step. Then these species can interact to generate the electronically excited state, which decays back in the form of emission. ECL generation through annihilation can be summarized as follows (eqs 1−6; Figure 1d), where $^1A^*$ and $^3A^*$ symbolize the species in singlet state and species in triplet state, respectively.[64] Based on the energy of the system, the emission of light occurs through different routes, such as the S-route, T-route, and ST-route. Some requirements must be fulfilled for the generation of efficient ECL through the ion annihilation pathway, including: (1) precursor molecules should show stable radical ions in the electrolyte of interest, usually checked with the help of a cyclic voltammetric (CV) response; (2) electron transfer reaction should demonstrate better photoluminescence (PL) efficiency of a product, that is commonly checked after conducting fluorescent experiments; and (3) there should be enough energy in the electron transfer reaction for the excitation of the required molecule as described above.[61]

2.2.2. Coreactant Pathway. Currently, all commercially utilized ECL analytical instruments successfully use a coreactant pathway. Thus, it is particularly important to understand the ECL mechanisms. Unlike ion annihilation ECL, the coreactant pathway utilizes a single oxidation/reduction step in the presence of a luminophore (emitter) containing solution by adding another reagent (coreactant).[65] On the basis of the polar nature of the applied potential, both coreactant and luminophore species undergo different oxidation or reduction reactions to emit light. The coreactant pathway is then divided into two types: one is oxidative−reductive ECL, and the other is reductive−oxidation ECL. The coreactant ECL exhibits several superiorities as compared to the annihilation ECL: (1) generation of ECL can be achieved in aqueous media at low potentials; (2) a single step oxidation/reduction ECL process that can be used for luminophores which exhibit only one reversible oxidation or reduction; (3) display of stronger ECL intensity; (4) negligible oxygen quenching effect.[66]

2.2.2.1. Oxidative−Reductive ECL. In oxidative reductive ECL, the oxidation of the coreactant generates highly reactive reducing intermediates. Oxalate ion ($C_2O_4^{2-}$) was the first coreactant discovered for ECL studies. Later, $Ru(bpy)_3^{2+}$ was utilized with $C_2O_4^{2-}$ to construct a new system for ECL studies as shown in eqs 7−13 in Figure 1d. In this system, the oxidation of $C_2O_4^{2-}$ resulted in the formation of a strong reductant $CO_2^{\bullet-}$, instead of an oxidant.[67] The most popular and widely studied $Ru(bpy)_3^{2+}$/tripropylamine (TPrA) system is another example of the oxidative reductive system that provides the basis of the commercial ECL applications. As shown below, the ECL is generated from oxidative reductive route (eqs 14−18; Figure 1d).[68] The ECL mechanism showed that both TPrA and $Ru(bpy)_3^{2+}$ undergoes oxidation process at the surface of electrode, and lately $Ru(bpy)_3^{3+}$ undergo reduction by TPrA● to generate the excited state.[69]

2.2.2.2. Reductive−Oxidative ECL. In the reductive oxidative mechanism, reduction of the coreactant generates strong oxidizing intermediates. Persulfate ($S_2O_8^{2-}$) is the first reductive oxidative coreactant developed for the $Ru(bpy)_3^{2+}$ based ECL studies, and the mechanism for light generation can be summarized as follows (eqs 19−24; Figure 1d).[70] Usually, ECL in reductive oxidative systems requires negative potential for the generation of the excited states. Therefore, hydrogen evolution causes serious trouble in observing a stable ECL response at extremely negative potentials in aqueous media.

https://doi.org/10.1021/acsmeasuresciau.3c00052
ACS Meas. Sci. Au 2024, 4, 3−24

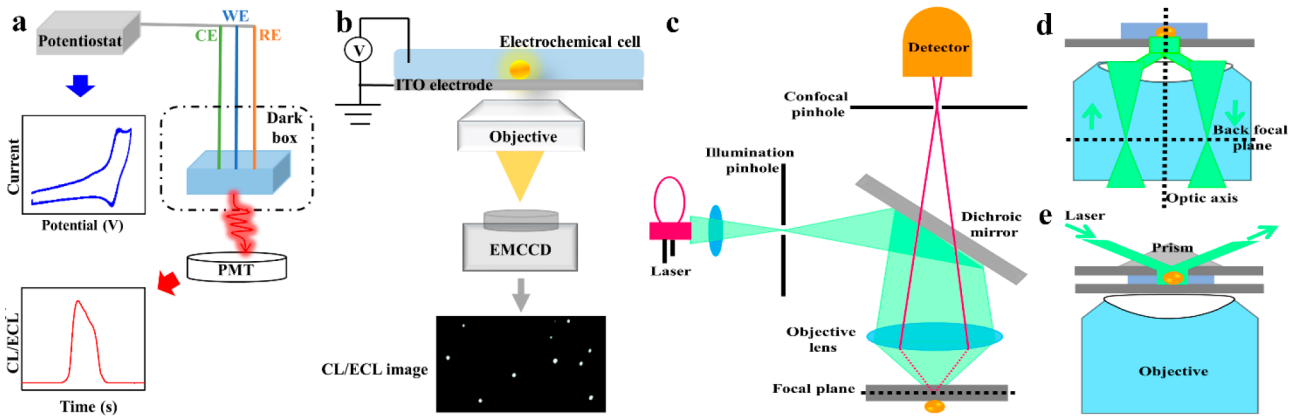

Figure 2. (a) Schematic of the typical CL and ECL light intensity (setup) based detections and (b) CL and ECL microscopy-based detection/imaging setup for single particle detection. Note: CL based detection/imaging does not require an electrochemical workstation (potentiostat). Schematic drawing of confocal microscopy setup (c), objective-type TIRFM setup (d), and prism-type TIRFM setup (e).

Carbon paste and bismuth electrodes and mixed solutions were utilized for cathodic ECL in aqueous solutions to overcome the hydrogen evolution problem.[71]

2.3. Light Generation Pathway in PL

PL is a phenomenon in which molecules/substances absorb ultraviolet or visible light to get promoted to the electronic excited state and emit electromagnetic radiation in the visible region while they decay back to the ground state (HOMO−LUMO transitions) (Figure 1e).[72] Such types of processes have been illustrated by a Jablonski diagram (Figure 1f), which could conveniently reveal photophysical processes and their corresponding lifetimes or kinetics. In this diagram, the energetically lowest electronic excited states can be symbolized as singlet (S_1) and triplet (T_1), while S_0 represents the singlet ground state. The singlet/triplet terms are used to denote the electronic state spin multiplicity. When a molecule/substance returns from an excited singlet state to the ground singlet state without changing the spin of excited state electron ($S_1 \rightarrow S_0$), it is called FL.[73] The difference between emission and absorption band maxima is called the Stokes shift. It is also regarded as an allowed transition, as no change occurs in electron spin. Therefore, the process of FL is quite fast, and the lifetime of the excited state is in the range of 10^{-8}−10^{-6} s. Through a spin conversion (flip), the molecules can undergo a nonradiative transition from S_1 to T_1, which is known as intersystem crossing (~10^{-9} s). On the other hand, in phosphorescence, the spin of the electron is inverted in the excited state and the excited triplet state decays back to the ground singlet state ($T_1 \rightarrow S_0$). This type of transition is less likely than a singlet-to-singlet transition, so it is also called a forbidden transition. As a result, the excited triplet state has a much longer lifetime (10^{-4} s and several seconds) compared to the corresponding singlet state. Phosphorescence usually has longer wavelengths as compared to FL, because the energy first excited triplet state is lower than the corresponding singlet state. Among CL, FL, and phosphorescence, the excitation process is different, but the emission spectra of an emitter are identical.[72]

As several types of molecules and materials display high FL quantum yields and optical filters can effectively filter out background scattering, FLM is the oldest and extensively used optical approach for imaging/analyzing single particles with high SNR. Since 1990s, several kinds of particles have been investigated for their (electro)chemical activities and photophysics.[2] Notably, nanomaterials demonstrate various key superiorities over molecules in FL imaging including improved photostability, large Stokes shift, long lifetime, large absorption cross section, and structure-dependent spectrum. To date, three types of mechanisms have been established for practical applications: (i) intensity based (blinking, quenching or enhancement); (ii) spatial superlocalization based; and (iii) spectrum based (anisotropy, lifetime, and wavelength).[2]

3. FUNDAMENTAL APPARATUS

3.1. CL and ECL Apparatus

Due to the absence of an excitation light source, the setups of both CL and ECL-based detection and imaging are simple.[26] For intensity based single particle detection, typical setup involved a custom designed transparent bottom (electro)chemical cell, electrodes, a photomultiplier tube (PMT), a dark box, and an electrochemical workstation (Figure 2a).[74] It is important to mention that both CL and ECL based measurements can be performed on a single instrument. In the case of CL, the light generation can be observed without using an electrochemical workstation. For CL/ECL based imaging applications, microscopes equipped with an objective, an EMCCD, and a few other optical elements are required in addition to setup items (Figure 2b).[75,76] In general, CL/ECL microscopes are structured into upright and inverted microscopic configurations.

The inverted microscopes avoid direct contact of the objective with electrolytes, while upright microscopes usually use water immersion objectives. However, upright configuration usually leads to limited magnification and spatial resolution.[34] Moreover, a high numerical aperture (NA) objective and a sensitive EMCCD camera are two crucial components for improving the light collecting efficiency and enabling single-photon detection (high-spatial-resolution CL/ECL imaging), respectively. It is important to mention that diffusion (not attached to the sample) of the luminophore (and ECL intermediates) can cause delocalization between CL/ECL and bright-field images, affecting spatial resolution. Therefore, most of the current CL/ECL imaging approaches show spatial resolutions up to a few micrometers. In contrast, the capability to achieve nanometer-level resolution is still a challenging task.[34] To achieve the visual detection of particles (not requiring spatial distinction), a mobile phone, digital camera, or simple CCD is enough to image the emission intensity. The digital camera could be applied for multiple CL/ECL detections. The developments in electrode architectures, novel potential

https://doi.org/10.1021/acsmeasuresciau.3c00052
ACS Meas. Sci. Au 2024, 4, 3−24

Table 1. Decision Table Showing the Comparison between CL, ECL, and PL Microscopy[35a]

	CL microscopy	ECL microscopy	PL microscopy
Sensitivity	☑☐☐ Chemical induced emission	☑☑☑ Electrochemical induced emission	☑☐☐ Photochemical induced emission
Sample stability	☑☐☐ Chemiluminescent reagents may modify the sample	☑☐☐ Coreactants in high concentration may modify the sample	☑☑☐ Excited light may modify the sample
Matrix effects	☑☑☑ Absence of light source	☑☑☑ Absence of light source	☑☐☐ Autobleaching and scattering effects
Spatial resolution	☑☐☐ Reaction products may diffuse before the CL reaction	☑☑☐ Strongly connected with the CCD detector	☑☑☑ Strongly connected with microscope setup and CCD detector
Spatial and temporal control	☑☐☐ Controlled by the chemical's addition	☑☑☑ Controlled by the applied potential and localized at the working electrode	☑☑☐ Controlled by the light source

[a]One, two, and three ticks indicate distinct levels of application or significance to each technique (e.g., one tick shows lowest importance, while three ticks shows highest relevance).

protocols, and sensitive emission capturing tools will continue to promote single particle detection applications.

3.2. FL Apparatus

Epifluorescence (wherein both the illuminated beam of light and emitted beam of light pass through the same objective lens) has been widely used in bio/biomedical imaging, but the SNR is not usually high enough for single particle detection. With certain approaches (reduced background signal), such as nanoconfinement,[77] single particle detection imaging can be achieved. More sensitive and advanced FL-based approaches can be generally categorized into two representative configurations: confocal microscopy (Figure 2c) for point-scanning imaging and total internal reflection fluorescence microscopy (TIRFM) (Figure 2d, e) for wide-field imaging, respectively.[73,78] Although confocal microscopy utilizes conjugate pinholes to eliminate the defocused (out-of-focus) signals for high SNR 3D imaging (e.g., accurate surface profiles and clear in-focus surface information on a particle/object), the scanning mechanics limits its real-time applications. Confocal microscopy is frequently opted for imaging thick biological samples, while TIRFM is favorite for single particles/molecules (sparsely distributed) detection/imaging with high SNR. In TIRFM, the incident excitation light undergoes a total internal reflection process on the interface of two different media.

TIRFM utilizes the concept in which a beam of light reaching the interface from high refractive index media into low index media (e.g., water (1.33, n_1) and glass (1.52, n_2) with an incident angle surpassing a specific critical angle ($\theta = \arcsin(n_1/n_2)$, that light beam is totally reflected. This reflection produces an evanescent wave (thin electromagnetic field) that propagates into the distal medium. The strength/ depth of evanescent wave depends on the refractive index differences, wavelength, and incident illumination angle, and its intensity decays exponentially with distance from the interface.[78]

Due to the near-field (limited region) characteristics of the evanescent field (<200 nm), selective illumination of molecules (at a single focal plane) can be achieved near the coverslip surface (liquid/solid interface) with enhanced SNR, making TIRFM an ideal tool for the detection/analysis of single molecules/ particles.

Both objective-type and prism-type setups (Figure 2d, e) can be utilized for TIRFM imaging; however, objective-type TIRFM demonstrates more dominance for single-molecule/particle studies. Moreover, the whole image can be acquired at a high acquisition speed due to the absence of laser scanning. In addition, high spatial (~10 nm) and temporal resolution can be achieved by combining TIRFM with super-resolution localization techniques.[2,78]

4. COMPARISON OF DIFFERENT LUMINESCENCE IMAGING TECHNIQUES

Choosing the appropriate luminescence microscopy for single particle imaging/detection and characterizing/visualizing the catalytic materials is not only useful for designing, optimizing, and developing high performance catalytic materials but also helpful for bringing new findings to surface science and (bio)analytical applications. To this end, it is crucial to understand the capability and shortcoming of each luminescence microscope (Tables 1 and 2). Moreover, luminescence (optical) microscopies show various inherent superiorities such as operation under ambient conditions, nondestructiveness to soft materials, straightforward and convenient planar glass cell/device preparation, easy accessibility and availability of the equipment, compatibility with different environments and reaction media, capability for in situ measurements, nanoscale spatial resolution, and so on.[18] In addition, super-resolution luminescence microscopies could further expand the resolution problem for probing single particle/molecule reactions.[79,80] Broadly speaking, super-resolution CL and ECL microscopies are still emerging techniques for probing single particle reactions as compared to super-resolution FL microscopy. These luminescence microscopic techniques may yield many new research opportunities in the near future.

5. SINGLE PARTICLE DETECTION/IMAGING

Revealing the structure−function relationships of functional materials enable exciting applications in heterogeneous catalysis, clean energy, and chemi-/biosensing.[2] It provides a strong basis for rational design of excellent materials by tuning their physicochemical properties (understanding the structural basis). To resolve the inherent structure and function inhomogeneity, single particle imaging/detection is emerging as a powerful complement to ensemble methods.[26] Recently, luminescence-based detection and imaging of individual nano/microparticles has been an area of hot research.[35] By utilizing superiorities of optical microscopy, numerous types of single nanostructures (NPs, nanocrystals, nanorods, nanotubes, quantum dots, and so on) with diameter of 10−100s nm can be visualized using high spatial resolution luminescence microscopies.[34]

Luminescence approaches have been performed to construct novel sensing platforms, visualize catalytic reactions, track motion of particles, and reveal energy applications of individual

https://doi.org/10.1021/acsmeasuresciau.3c00052
ACS Meas. Sci. Au 2024, 4, 3−24

Table 2. Comparison of CL, ECL, and FL Microscopic Techniques for Detection/Imaging of Single Particles

technique	capabilities	shortcomings	remarks for future development	ref
CL microscopy	Imaging of single particles; study of structure−activity relationships; tracking/ visualizing single microswimmers; single bead based (bio) analysis	Limited photon flux (low CL quantum yield); low light emission level of single particles; poor control over CL reactions; require a CL nanoemitter/ luminophore	Efficiency of CL microscopy could be enhanced by designing/ developing highly emissive particles, bright/ tunable chemiluminescent molecules (probes), effective microscopic configurations/ set-ups, and highly sensitive light collection tools	26, 29, 38, 39, 49, 81
ECL microscopy	Determination of the structure-dependent electrocatalytic activities of single nanocatalysts; Imaging of the facet-dependent heterogeneities of single particles; stochastic collision electrochemistry; visualization/ monitoring of catalytic reactivities (e.g., HER, OER) of single NPs; single bead (bio)analysis	Require an ECL luminophore/ nanoemitter; low ECL efficiencies of single particles	Performance/applicability of ECL microscopy could be further improved in electrocatalysis and visualization of individual particles/molecules reactions by designing/ developing strong nanocatalysts, highly effective and stable nanoemitters/ luminophores, and using highly sensitive light emission collection tools; moreover, super-resolution ECL microscopy could improve the resolution limits for visualizing single particle/molecule reactions	27, 46, 48, 76, 82−87
FL microscopy	Study nanocatalysis (e.g., photoelectrocatalysis, electrocatalysis) of single NPs/molecules; imaging, sensing, and tracking of fluorescent nanomaterials; collision/oxidation of single NPs; single molecule sensitivity; single bead (bio)analysis	Usually suffered from photobleaching; limited availability of fluorescent dyes; require a fluorophore	Synthesis/discovery of new fluorescent particles/molecules, electrode surface modification with highly catalytic materials, transduction of suitable FL systems with (electro)chemical approaches, and capacity to study nonfluorescent reactions could further extend/improve the applications of FL microscopy; more importantly, super-resolution FL microscopy could further expand resolution limits for studying individual particles reactions	6, 20, 44, 88−95

particles. Moreover, nano/microfabrication of devices and microelectrodes significantly improves mechanistic studies and ultrasensitive sensing.

5.1. Static Single Particles

Measurements on a single particle or single site level could precisely reveal structure−activity relationships, dynamic information, environment-influenced chemistry, and heterogeneity of nanoscale structures. CL-based imaging of single particles is a highly challenging task because CL reactions mostly accompany limited photon flux. In FL imaging, an individual fluorophore undergoes rapid excitation−relaxation cycles to repetitively emit up to one million photons. In contrast, an individual molecule reaction can release only a single photon (CL quantum yield = 1) under the best experimental conditions. As a result, it is quite challenging to achieve sufficient SNR for single particle imaging because a particle may not accumulate the necessary photon numbers due to the small quantity of CL molecules.

The Cui and Wang groups demonstrated the first CL (optical) imaging technique to demonstrate the light generation capability of single magnetic-polymer microbeads functionalized with a luminol analogue (*N*-(4-aminobutyl)-*N*-ethylisoluminol (ABEI)) and cobalt (II) (Co^{2+}) (Figure 3a).[26] The authors first monitored the CL reaction kinetics and imaging of an individual particle under the reaction conditions. Two subpopulations by real-time imaging of multiple particles were successfully distinguished (Figure 3b), which shows strong and weak CL signals, respectively. Additional characterizations with scanning electron microscopy (SEM) and confocal fluorescence microscopy (CFM) were performed to resolve multicore (amorphous) structures, which were leading to delayed and strong CL signals. It was demonstrated that this kind of structures could significantly improve CL intensity and kinetics due to the optimized accessibility of H_2O_2, enhanced chemical activity of ABEI and Co^{2+}, and improved encapsulation efficiency toward ABEI molecules.[26] This study provided a novel platform to draw a clear structure−function relationship, which was readily applied for designing high performance microbeads. The high performance of this approach was validated by CL assay at an ensemble and CL imaging at an individual particle level.

Both experiments proved that rationally designed microbead batches (Figure 3b) showed improved analytical performance (2,4,6-trinitrotoluene detection with low detection limit (improved by 53 times), extended dynamic range (2 orders of magnitude expanded)) and enhanced CL emission. This work successfully revealed structure−function relationships using CL imaging and validated the role of single particle detection for designing and developing high performance functional materials for practical analytical applications.

Single NP detection using ECL microscope was first described by Bard and colleagues.[96] The newly developed method was used to image the ECL emission of single NPs of a conjugate polymer (r = 25 nm), F8BT, using TPrA as a coreactant. This study revealed dynamic information about the ECL process, heterogeneous kinetics (electron-transfer rate), and mechanism at an individual particle level that cannot be obtained from ensemble measurements.[96] Over the last few decades, super-resolution techniques have revolutionized the field of FLM. Very recently, Zhao and co-workers first proposed super-resolution ECL microscopy to image the site- and facet-specific electrocatalytic activities of individual NPs (2D Au nanoplates, 1D Au nanorods (NRs), Au nanospheres) with

https://doi.org/10.1021/acsmeasuresciau.3c00052
ACS Meas. Sci. Au 2024, 4, 3−24

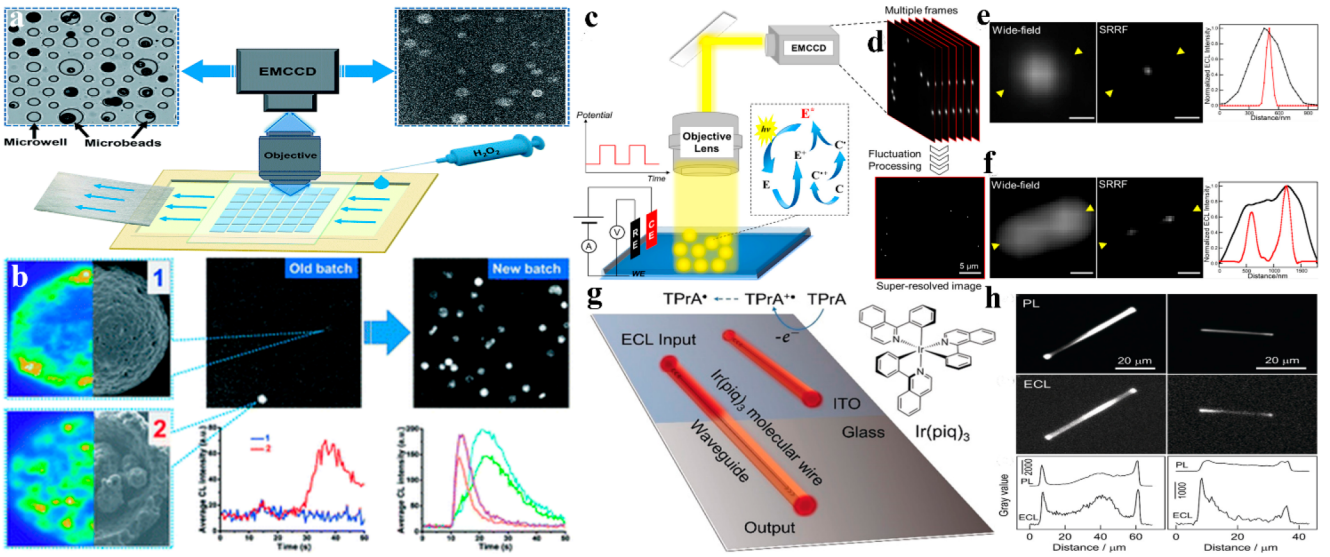

Figure 3. (a) CL-based imaging setup designed for detecting and imaging single microbeads. (b) Representative CL kinetic curves (left panels) and averaged CL images (right panels) from the old and new batches of microbeads during reaction with H_2O_2, respectively. Reprinted from ref 26 with permission from the Royal Society of Chemistry, copyright 2019. (c) Schematic showing the single particle imaging with ECL microscopy setup. E symbolizes the luminophore ($Ru(bpy)_3^{2+}$), while C represents the coreactant (TPrA). (d) SRRF analysis (basic principle) of multiple frames (images). (e, f) Wide-field ECL images (left panels), super-resolution ECL images (middle panels), and corresponding line profiles (drawn from the areas/regions between yellow-colored arrowhead) of an individual Au nanosphere and separated Au nanospheres, respectively). Scale bar: 500 nm. Reprinted from ref 80 from American Chemical Society, copyright 2021. (g) Schematic drawing showing the ECL waveguide in an individual crystalline molecular wire of $Ir(piq)_3$ on an electrode surface (patterned ITO). (h) Representative PL (top), ECL (middle) images, and corresponding grayscale variations of two molecular wires along the longitudinal axis. Reprinted from ref 83 with permission from Wiley-VCH, copyright 2020.

nanometer resolution (Figure 3c–f).[80] The application of super-resolution radial fluctuation (SRRF) was evaluated in ECL imaging. During ECL reactions, the photons were generated in a stochastic way (independent of each other), which obeyed Poisson statistics. The temporal variations of the ECL emission intensities in consecutive frames were utilized to apply the SRRF algorithm for ECL image reconstruction. By processing (input) multiple frames for radiality transformation, a spatial resolution of ∼100 nm was achieved for ECL images, which revealed more detailed catalytic activities on a subparticle level. Beside traditional wide-field ECL imaging, super-resolution ECL microscopy not only uncovered defect- and facet-dependent surface reactivities but also revealed dynamic fluctuations of reactivity patterns on (within) individual NPs. This super-resolution approach holds strong potential in the areas of single-entity analysis, biological imaging, and catalysis.

In a recent report, the Su group first observed an ECL waveguide in an individual crystalline molecular wire.[83] An individual 1D crystalline molecular wire of tris(1-phenyl-isoqsuinoline-C^2,N)iridium (III) ($Ir(piq)_3$) displayed dual roles as both an active waveguide and ECL emitter (Figure 3g, h). ECL microscopy revealed a typical optical waveguide phenomenon, wherein the ECL emission was much brighter at the terminals. Importantly, the ECL generation was confined inside the molecular wires and propagated up to 100 μm along the longitudinal direction.[83] This work successfully demonstrated the capability for conducting contactless electrochemical analysis and studying chemical/ biochemical systems without or with less electric disturbance.

Besides, ECL holds immense potential to evaluate the catalytic properties of noble metal catalysts by recording their local redox activities toward generation of ECL. For example, Pan and colleagues studied the local redox activities of single gold (Au) NPs (with $Ru(bpy)_3^{2+}$-TrPA system) using the ECL microscopy coupled with voltammetry.[97] With increasing particle size (30 to 300 nm), ECL generation was also increased that was affected by the charge transfer and local chemical environment of NPs. Due to the rapid oxidation (under positive potential) of AuNP surface, the generated ECL emission exhibits limited stability.[97] Similarly, the Willets group achieved ECL imaging at single gold nanowire electrodes (microsized).[98] The gold nanowires were coated with a polymer blend (PEDOT: PSS–PVA) to enhance their protection against electrochemical damage and surface oxidation. It was revealed that polymer thickness can enhance ECL reproducibility during multiple redox cycles and improve the ECL image (sharpness) quality.[98]

FL microscopy is a potential approach for studying catalysis and dynamic collision and oxidation of NPs on an individual molecule or particle level through fluorogenic reactions. In these experiments, NPs can catalyze nonfluorescent reactants to produce strong fluorescent products, providing the basis for subsequent detection and imaging at a single particle/molecule level.[88] Typically, fluorescent NPs are embedded within a condensed phase matrix or sparsely dispersed over a support. After the laser beam induced excitation, the product generated FL is accumulated using the objective of the microscope and further projected onto a camera (EMCCD). By recording stochastic events (e.g., FL bursts) at a single particle level, time trajectories of FL intensity, single catalytic turnover, and reaction kinetics (τ_{off} and τ_{on} times) can be achieved. FL imaging demonstrate various advantages for studying such reactions including single-active-site or single- particle resolution, single reaction temporal resolution (high sensitivity), wide-field imaging enabled parallel observation of multiple particles, in situ/ operando measurements, and super-resolution imaging based 10–100s nm localization accuracy. Based on all these excellent characteristics, single molecule FLM has been

https://doi.org/10.1021/acsmeasuresciau.3c00052
ACS Meas. Sci. Au 2024, 4, 3–24

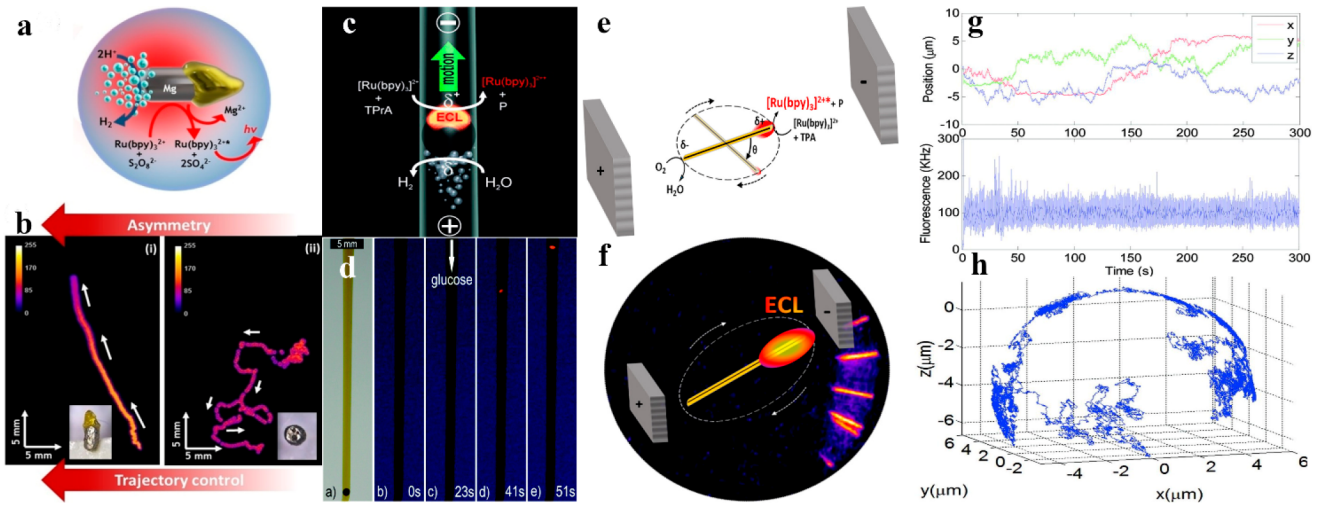

Figure 4. (a) Schematic displaying the motion and CL generation principles of an autonomous chemiluminescent Janus microswimmer. (b) Tracks imaging reveals the maximum CL emission of an anisotropic CL particle modified with a polymer (i) and unmodified isotropic particle (ii) moving at a solution surface. The solution was prepared by mixing H_2SO_4 (20 mM), $K_2S_2O_8$ (20 mM), and $Ru(bpy)_3(PF_6)_2$ (1 mM) in H_2O/ACN (1/1). Global time: 90 s (every experiment). Adapted from ref 81 with permission from the Royal Society of Chemistry, copyright 2020. (c) Asymmetric redox activity on the surface of a bipolar swimmer induced its simultaneous motion and ECL emission in a glass tube. Reprinted from ref 100 with permission from Wiley-VCH, copyright 2012. (d) Images displaying dynamic glucose detection, wherein ECL was switched on during the swimmer motion (toward top of the capillary) in a vertical glucose concentration gradient. Reprinted from ref 101 with permission from the Royal Society of Chemistry, copyright 2014. (e, f) Image displaying ECL tracking (spatial distribution) of a magnetic rotating BPE. Reprinted from ref 82 with permission from American Chemical Society, copyright 2019. (g) 3D tracking (x, y, z positions; top panel) of a PS particle (diameter ~ 200 nm) and corresponding FL intensity while diffusing at a silicone oil droplet (surface) in water. (h) 3D trajectory displaying the oil droplet profile. Reprinted from ref 105 from American Chemical Society, copyright 2012.

extensively applied for uncovering shape and size effects (such as plasmonic metal NPs, metal nanoclusters, carbon nanotubes (CNTs) and dots, polymer dots, perovskite QDs, up-conversion nanomaterials and so on),[2,10] mapping the distribution of active sites, imaging dynamic collision events, and probing heterogeneous reaction pathways for single particles.[6]

5.2. Single Particle Swimmers

Controlling the movement of micro- and nanodevices and small particles (microswimmers) is important for several fields, including nanomedicine, micromotors, and DNA assays or dynamic multiplexed immunoassays. Self-propelled chemiluminescent single microswimmers present a new concept for tracking and visualizing active objects. Interestingly, self-propelled systems have shown potential applications in the areas of analytical chemistry (sensing), environmental remediation, and biomedical research.[99] For example, Kuhn and colleagues developed two distinct types of self-propelled CL swimmers. In the first work, Prussian Blue filled alginate hydrogel beads (Janus particles) display chemical light emission coupled with dynamic oscillatory behavior.[99] A symmetry breaking approach was applied to transform Prussian Blue beads into Janus particles using an electric field. The differential porosity distribution of the hydrogel particle caused an asymmetric release of oxygen (O_2) bubbles, which triggers motion (propel) of the particle. Prussian Blue simultaneously catalyzed both oxygen production and light emission with the addition of luminol-H_2O_2.

In the second work, the authors designed an autonomous chemiluminescent Janus microswimmer by utilizing asymmetrically modified magnesium (Mg) microparticles as an active ingredient.[81] These (janus) microparticles/ microswimmers were synthesized by utilizing a straightforward bipolar electromilling method (particle shaping), followed by indirect bipolar electrodeposition (asymmetric modification). The as-designed Janus particles were simultaneously moving (bubble propulsion mechanism) and generating CL by triggering the redox reactivities between Mg, $Ru(bpy)_3^{2+}$ and $S_2O_8^{2-}$ (reductive-oxidation reactions) (Figure 4a). By using these phenomena, the degree of asymmetry was directly correlated with the directional motion of the synthesized particles (Figure 4b). These autonomous chemiluminescent swimmers may find broad applications in sensing (e.g., observing CL quenching with the addition of specific targets), real-time tracking of motion, studying collective behavior (e.g., schooling and swarming) of swimmers, and understanding/ revealing interswimmer communications.

Sojic and colleagues proposed an innovative bipolar electrochemical approach, wherein a single conducting particle (swimmer) was simultaneously moving (gas bubbles propulsion) and generating ECL emission.[100] Simultaneous reduction and oxidation (asymmetric electroactivity) of H_2O and ECL reagents at the cathodic and anodic poles induced the motion and ECL generation from the glassy carbon beads in a U-shaped capillary cell (Figure 4c). The polarization voltage displayed a proportional trend between the diameter of the bead and external electric field induced on the bead. The speed of the swimmers is affected by the bubble formation and collapse rate.[100] The authors applied the same concept of ECL swimmers driven by bipolar electrochemistry for dynamic enzymatic glucose sensing (Figure 4d).[101]

ECL is a 2D process, wherein emission of light is generated only at the surface of the electrode (strictly confined). Kuhn and Sojic groups first developed a 3D ECL approach using bipolar electrode (BPE) to generate emission from millions of nano- or micro-objects (microemitters) dispersed in bulk solution.[102] Each single object (multiwalled carbon nanotube or microbead) was controlled in a wireless manner, and they emit ECL

https://doi.org/10.1021/acsmeasuresciau.3c00052
ACS Meas. Sci. Au 2024, 4, 3−24

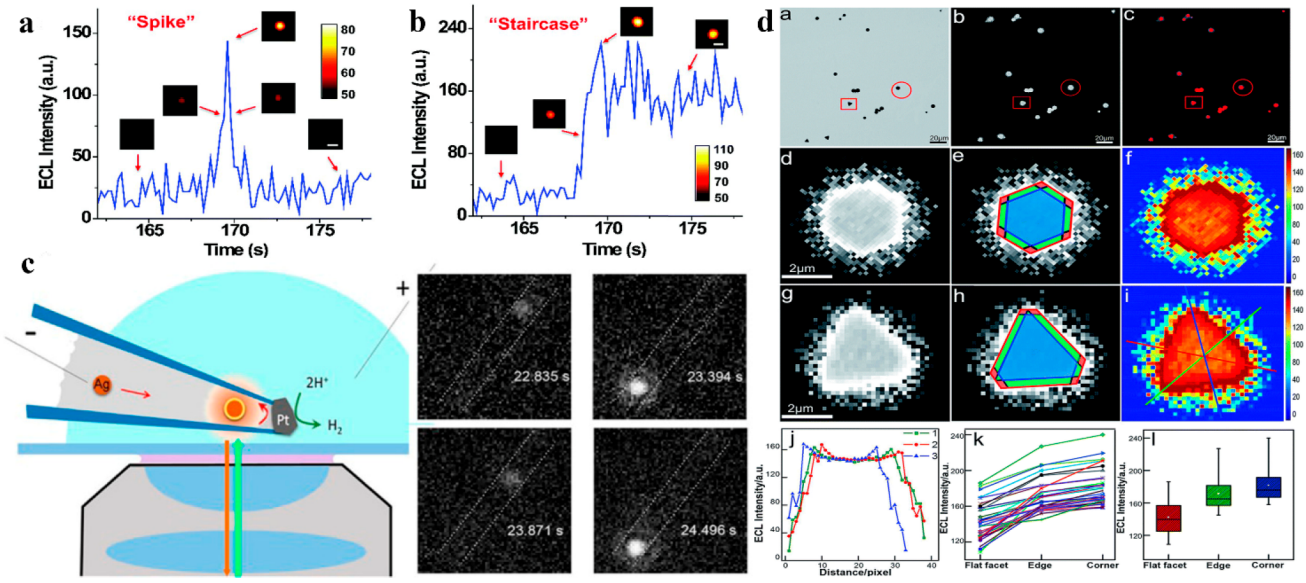

Figure 5. Single NP collisions generated discrete ECL signals: (a) "spike" and (b) "staircase." Inset: ECL images of a single NP during collision events. Exposure time: 0.2 s; scale bars: 2 μm; constant potential: 1.4 V. Reprinted from ref 85 with permission from the Royal Society of Chemistry, copyright 2018. (c) Schematic illustration of the experimental setup utilized for FL imaging of single Ag NP collision events inside a microfabricated nanocell (nanopipette) (left column). FL images represent the individual particle collision responses under different time periods (right column). Reprinted from ref 89 from American Chemical Society, copyright 2017. (d) A series of images showing the spatial distribution of ECL intensities on an individual Au nanoplate. Representative bright-field (a), ECL (b), and corresponding false-color overlay image (c). Enlarged version of red circled areas (d, g) of the ECL image (b). Divided regions of flat surface facet (blue), edges (green), and corners (red) in (e, h) ECL images. Matlab obtained ECL intensities with a 2D spatial distribution (f, i). ECL intensity gradients (j) for three recording lines shown in (i). Statistical and box charts illustrate site-specific ECL intensities. Reprinted from ref 46 with permission from the Royal Society of Chemistry, copyright 2019.

collectively in the solution. As a result, the whole solution (entire volume) produced ECL emission. This kind of bulk ECL emission could make several new openings in optical tracking of nanomotors and as high-sensitivity ECL analysis.[102]

This concept was further applied for the dual enzymatic detection of choline by applying the luminol/ choline oxidase system and glucose with the $Ru(bpy)_3^{2+}$/glucose dehydrogenase system, respectively.[103] The authors selectively and simultaneously detected these analytes over extended concentration ranges. In a recent work, the same group designed an innovative double-remote system by a synergetic combination of electric and external magnetic fields (Figure 4e, f).[82] These fields induced the rotational motion (magnetic field) and bipolar polarization (electric field) of a gold-coated iron wire (length ~ 20 mm; diameter ~ 150 μm), wherein the latter triggered the local ECL generation that was utilized as an optical readout (ECL intensity variations) for tracking the electrode motion. The rotational motion generated convection effects that can enhance ECL emission. Theoretically, this object has strong similarity with a classical rotating electrode, but with wireless electrochemical addressing and contactless magnetic control. The developed method can enable exciting applications in designing multifunctional systems coupled with immunoassays or dynamic enzymatic detection.[82]

Single particle tracking (SPT) is an emerging approach to analyze and observe the motion and position of individual particles/molecules, enabling quantitative mechanistic information in complicated systems that cannot be achieved using traditional ensemble-based approaches.[104]

The motion of particles can be quantitatively analyzed by considering the local extent or step size of confinement, instantaneous velocity, and diffusion coefficient. Such characteristics could uncover the interaction between the tracked particles and their local surroundings. FLM is a powerful technique to track, locate, and visualize single particles in a diverse range of complex systems (e.g., biological systems).

For example, Berglund and colleagues studied 3D single fluorescent NPs (size 24−2000 nm) transport dynamics with real-time feedback control at a silicone oil−water interface (Figure 4g, h).[105] The smaller particles exhibited an unusual enhancement in drag force at interface, while larger (>200 nm) particles diffusion coefficient scaled inversely with particle size. The obtained results revealed the applicability of real-time 3D tracking for exploring in situ dynamics (three-phase line tension, interface curvature, charge-induced interface deformation, and variation in surface functionality) of interfacial NPs with high spatiotemporal resolution in 3D geometries. This technique holds great potential for studying 3D dynamics in complex systems such as geological media, biological cells, gels, complex fluids, and other intrinsically 3D materials. Several studies have shown that 3D-SPT can be successfully applied for a broad range of targets such as single quantum dots,[106] single Au NPs,[107] single molecule tracking,[108] and so on.

5.3. Single Particle Impact, Collision, and Oxidation

Single particle studies using electrochemical approaches have been extensively documented for analyzing NPs, in addition to studying the electron transfer and interfacial charge processes. For example, the Bard group studied the collision events of water/oil suspended single droplets at the surface of ultramicroelectrodes (UMEs).[109−111] ECL emission transients and amperometric current (i−t curves) transients were simultaneously observed to detect single attoliter droplet collisions in a water/oil emulsion.[109] The authors formed an emulsion system based on droplets of (1:2 v/v) TPrA and toluene, suspended in water using ultrasonication and emulsified by ionic liquids. When rubrene (ECL luminophore) was introduced to the

https://doi.org/10.1021/acsmeasuresciau.3c00052
ACS Meas. Sci. Au 2024, 4, 3−24

emulsion droplets, stochastic events were monitored by measuring both the oxidation currents (blips) at the surface of UME and the follow-up reactions that produced ECL blips. Therefore, this study enabled two different (electrochemical and ECL) simultaneous observations for tracking single emulsion droplets (micro- and nanosized), and detection/analyzing of their sizes and contents.[109] The same group also described a novel method for characterizing single particle (PtNP with diameter of ∼4 nm) collision events by catalyzing the oxidation (amplified ECL) of $Ru(bpy)_3^{2+}$-TPrA ECL pair.[112] Each collision event resulted in a distinct photon spike, whose frequency and amplitude could be associated with the concentration and size of particles. By using a higher concentration of ECL pair and selecting a suitable electrode, a significant amplification in ECL emission could be achieved. This work holds enormous potential for studying heterogeneous electron-transfer kinetics and dynamics of the processes at an individual particle level.[112]

Detailed understanding of the reactivity process at phase boundaries is crucial to diverse chemistry fields ranging from heterogeneous catalysis to synthesis. To achieve this target, Dick and Glasscott visualized the phase boundaries of multiphase systems using ECL imaging on a glassy carbon electrode (GCE).[113] By adjusting the solubilities of the $Ru(bpy)_3^{2+}$-oxalate pair in either the 1,2-dichloroethane (DCE) or water phase, the authors selectively imaged the 2D contact interface for a single water droplet (micrometer size). The microdroplet contact radii were quantified and visualized through selective mixing of the coreactant and luminophore in microdroplets of the water. The three-phase boundary thickness was quantified at a GCE/1,2-DCE/water interface through selective dissolving of the luminophore in the 1,2-DCE and the ECL coreactant in the water microdroplet continuous phase. The obtained results measured a 9 ± 3 μm interfacial thickness. Moreover, the electrogenerated O_2 bubbles growth dynamics were also revealed at water/gas interface.[113] Selectively imaging phase boundaries using ECL holds immense potential for investigating interfaces in various physical and chemical processes.

Besides observing single-particle impact based on intensity, ECL microscopy is also capable of visualizing the stochastic collision electrochemistry of single NPs. For instance, Zhu and colleagues studied stochastic collision electrochemistry at an individual ECL nanoemitter level.[85] Highly ECL emissive $Ru(bpy)_3^{2+}$-doped silica nanoparticles (RuDSNs) were synthesized with three varied sizes. This approach could spatially differentiate simultaneous collision events and trace 3D collision trajectories of single RuDSNs, which can provide high-throughput information about the kinetics of the NPs. Single RuDSNs collisions generated discrete ECL signals, which could be broadly categorized as spike (elastic collision) and staircase (sticking collision) (Figure 5a, b). Moreover, collisional ECL intensities, collision frequencies, and collision types of single-NPs were correlated with diffusion fluxes, particle concentrations, and interfacial properties. This approach displayed strong potential in single-particle analytical and electrochemical research applications.

Diverse range of functional materials have been widely exploited in (electro)chemical sensing, fuel cells and batteries, electrodeposition, and (electro)catalysis. The study of electron transfer rates on an individual NP level with respect to time or electrode potential is important for evaluating and determining their corresponding (electro)chemical reactivities. FLM is a leading technique for acquiring local (electro)chemical information through optical signals. Most importantly, optical detection of single-particle collision events is a fast-growing area due to its unique superiorities.[114] Although numerous types of NPs have been studied, oxidation of individual silver (Ag) NPs has received significant attention due to their superior applications in a range of research areas (e.g., catalysis, sensors, electronics, and so on) and their environmental effect and biological activity.[115] For instance, the Pan group combined methods of FLM and dark-field scattering (DFS) to investigate the optical spectroelectrochemical responses of individual Ag NPs.[116]

Although great progress has been made in single NP collision electrochemistry, a comprehensive study of the single NPs dynamics at the electrochemical interface has rarely been rarely reported. To tackle this challenge, the Zhang group developed an innovative method that allows imaging of colliding Ag NPs inside a microfabricated nanocell using a single-particle FLM.[89] By recording the FL intensity of the Ag nanocluster generated by the oxidative products (photocatalytic decomposition) of silver oxide (Ag_2O), the authors directly recorded (imaging) the dynamic collision events of a single Ag NP inside a nanoscale electrochemical cell as it collides at the electrochemical interface. The authors suggested that overall particle motion (repeated motion) was ascribed to the balanced electrostatic interactions between the positively biased Pt electrode, the NP, and charged quartz nanocell walls (Figure 5c). In another work, the same group also applied single-particle FLM to validate the production of Ag_2O during NP collisions (individual-collision event).[117]

5.4. Single Particle (Electro)catalysis

Heterogeneous catalytic processes play a crucial role in achieving a sustainable future due to their central importance in various energy and chemical industries. It is crucial to analyze/detect catalytic activities and corresponding mechanisms of single NPs for drawing structure−function correlations and subsequently designing high performance catalysts.[42,118] ECL microscopy offers a real-time and high-throughput analysis of electrocatalysis at single bimetallic catalysts. For instance, Xu and co-workers developed an ECL imaging approach to explore the catalytic oxidation of luminophore at an individual Au-Pt Janus, platinum (Pt), and AuNP.[48] It was shown that heterogeneous structure Janus particles displayed enhanced ECL stability and intensity compared to that of monometal NPs, suggesting superior electrocatalytic efficiency. By combined digital simulation and experimental results, it was revealed that two distinct faces of Janus particles (asymmetric bimetallic interface) lead to a fluid slip and concentration gradient around the particle, which could avoid the generation of oxidation layer and enhance mass transport velocity (local redox reactions).[48] The same group further visualized the catalytic reactivities of bimetallic one-dimensional (1D) Pd−Au NRs (diameter ∼ 20 nm; length ∼ 66 nm) at the single-particle level using ECL microscopy.[119] The two metals (Pd and Au) exhibited different electron transfer rate constants (heterogeneous), which showed distinct catalytic abilities and stabilities toward ECL generation. It was shown that Pd-tipped Au nanostructures (dog-bone-shaped) presented clearly stronger ECL emission, while Pd−Au Janus (two-faced) NRs demonstrated superior stabilities in comparison to that of homogeneous surface Pd-covered Au NRs and Au NRs (monometallic). This study helps in designing effective bimetallic nanocatalysis.[119] The same group further explored the electrocatalytic potential of single 2D gold

https://doi.org/10.1021/acsmeasuresciau.3c00052
ACS Meas. Sci. Au 2024, 4, 3−24

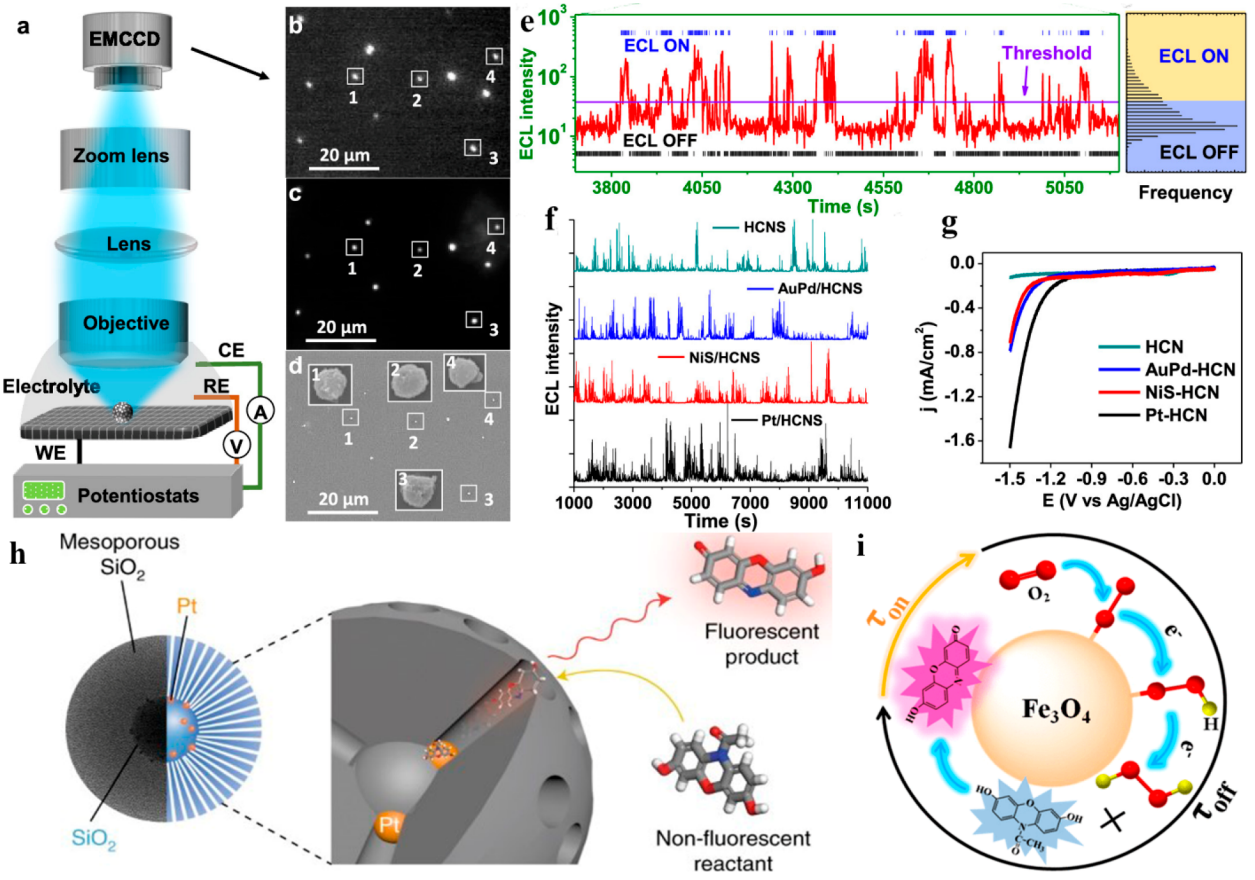

Figure 6. (a) Schematic showing the setup of ECL microscopy applied for monitoring HER at an individual NP level. Colocalization analysis of (b) ECL, (c) FL, and (d) SEM images of the same HCNSs sets. (e) ECL trajectory of a single HCNS during a constant (−1.5 V) negative potential. ECL OFF state (black stick marking) and ECL ON state (blue stick marking) were distinguished for statistical analysis by setting the threshold. (f) ECL trajectories of Pt-HCNS, NiS-HCNS, AuPd-HCNS, and pristine HCNS, at −1.5 V. K_2SO_4 (100 mM) solution containing $K_2S_2O_8$ (100 mM) coreactant was used as electrolyte. ECL and FL imaging exposure time was 1 s. (g) Resulting polarization curves for the HER at 5 mV/s (scan rate) in the K_2SO_4 (100 mM) electrolyte. Reprinted from ref 84 from American Chemical Society, copyright 2020. (h) Scheme showing a nanocatalyst image in nanoconfinement that consist of PtNPs (5 nm) sandwiched between a mesoporous SiO_2 shell (120 nm) and a solid SiO_2 core (100 nm). The nonfluorescent (AR) reactant molecule was oxidized (catalytically) at the PtNPs active surface sites to produce fluorescent (resorufin) product molecule. Reprinted from ref 127 with permission from Springer Nature, copyright 2018. (i) Schematic revealing the 2e ORR at a single Fe_3O_4 NPs level. Reprinted from ref 128 from American Chemical Society, copyright 2020.

nanoplates (microsized; diameter ∼1−4 μm) with good spatiotemporal resolution.[46] The corner, edge, and flat facets displayed heterogeneous ECL intensities, indicating site-specific catalytic reactivity on an individual nanoplate (Figure 5d). In comparison to super-resolution FLM,[6] real-time ECL microscopy achieved higher (millisecond scale) temporal resolution imaging, which could enable better understanding of single nanocatalyst reactivity patterns.[46]

Besides drawing structure and function relationships of nanocatalysts using classical ECL reactions of luminol (and its analogues)-H_2O_2 and $Ru(bpy)_3^{2+}$-TPrA systems, ECL microscopy can also behave as a potential (in situ) visualization tool to investigate crucial electrocatalytic reactions (e.g., mechanism information and surface reactivity) of particles related to clean energy conversion. For example, Zhu and colleagues first visualized the catalytic activity at individual quantum dots (QDs) level participated in water oxidation reaction using in situ ECL microscopy.[120]

By sweeping positive potentials, the catalytic active sites at QDs surface induced the formation of hydroperoxide intermediate OOH(ad), which could significantly increase the ECL intensity of luminol analogue as coreactants. The investigation of distinct types of QDs having different valence band positions, such as CdSeTe, CdTe, and CdSe was also performed. It was discovered that CdSeTe generated the strongest ECL emission due to an appropriate valence band position and more defects.[120] The same group further developed an effective method to in situ image/investigate the spatial heterogeneity of catalytic reactivity on different facets of zinc oxide (ZnO) crystal at a subparticle level using ECL microscopy.[76] Very recently, the same group first mapped the catalytic reactivity of an individual graphene sheet with a nanometer (400 nm) spatial resolution of ECL microscopy.[86] It was concluded that this high-spatial imaging depends on the stochastic ECL illumination due to the different adsorption rates of H_2O_2 at different graphene sheet surface sites.

Hydrogen evolution reaction (HER) is an environmentally friendly hydrogen gas generation process from water under mild condition reactions. To date, researchers use ensemble measurement approaches to identify/optimize the potential of HER catalysts, which record only the averaged response generated by various catalytic materials having different electroctalytic reactivities. The observation of HER activities on a single-NP or microscopic scale could reveal structure−

https://doi.org/10.1021/acsmeasuresciau.3c00052
ACS Meas. Sci. Au 2024, 4, 3−24

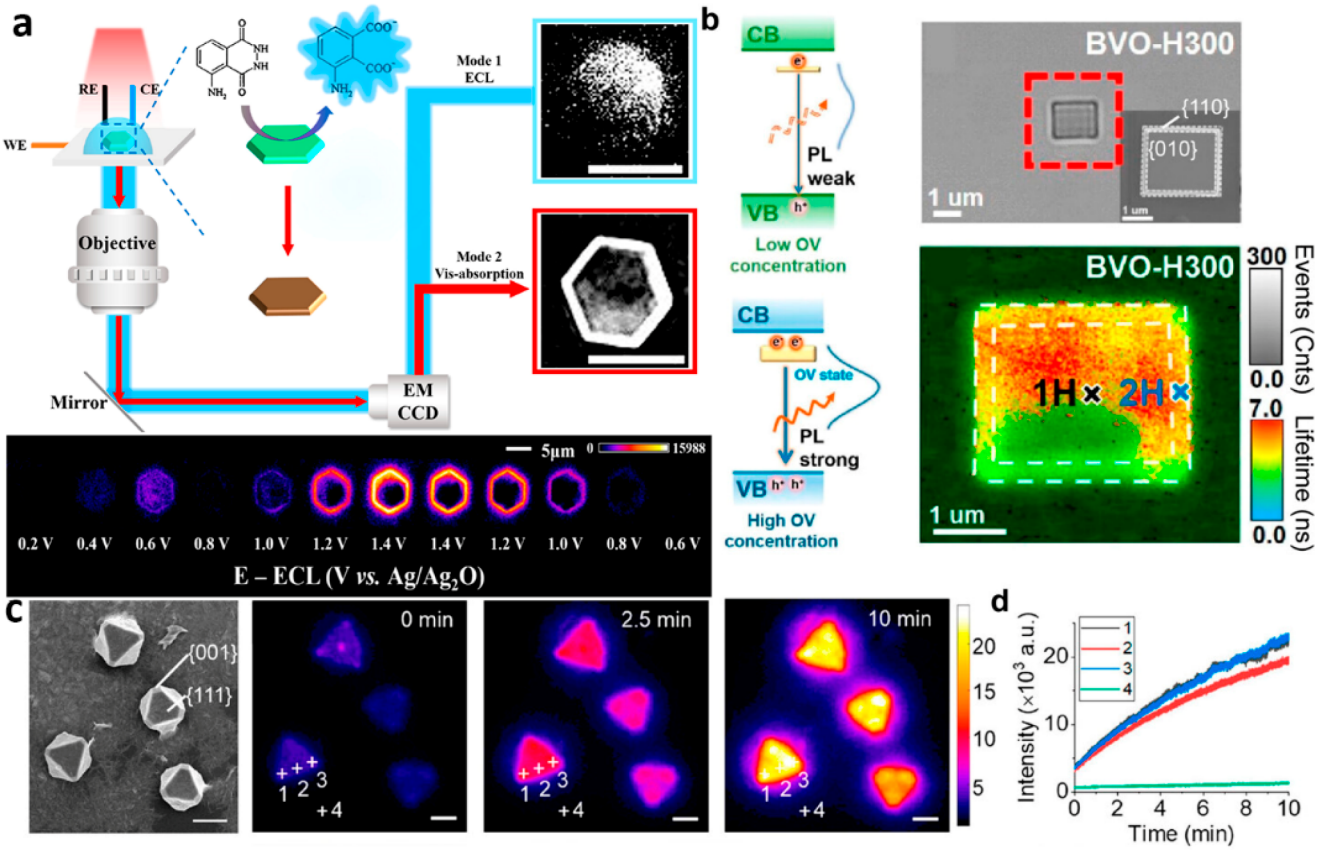

Figure 7. (a) Schematic showing the dual-mode imaging of a single nanoplate of the $Co(OH)_2$ OER process using Vis-Absorption and ECL. ECL imaging (bottom part) achieved under applied voltage from 0.4 to 1.5 V. Reprinted from ref 130 from American Chemical Society, copyright 2023. (b) Oxygen vacancies spatial distribution tracking across varying facets of a single $BiVO_4$ particle in an in situ manner. Reprinted from ref 131 from American Chemical Society, copyright 2023 . (c, d) PL images of single Cu_2O microcrystals over different periods of time for revealing their corresponding heterogeneous photocorrosion activity. Reprinted from ref 132 from American Chemical Society, copyright 2022, .

function heterogeneity among the individual particles. In a recent work, Lin and collaborative groups first identified HER activities of a single nanocatalyst using ECL microscopy (Figure 6a–g).[84] The authors developed a new ECL blinking approach to record the generation of H_2 nanobubbles from hollow carbon nitride nanospheres (HCNSs). The collapse, growth, and generation of H_2 nanobubbles were identified using the ECL ON/OFF states. The generation of H_2 molecules was further validated by gas chromatography. The duration of ECL OFF and ON states follow power-law distributions, which revealed multiple catalytic sites on an individual HCNS. Moreover, it was also revealed that ECL blinking could reduce the quantum yield (lower cathodic ECL efficiencies) of cathodic nanoemitters.[84]

Single molecule FLM can reveal structure–property relationship of single particles by imaging reactants/products and surface reaction hot spots of catalytic reactions at the level of an individual molecule/particle with nanometer precision.[121,122] Such information could be utilized for designing and developing high performance catalysts. For example, Xu and colleagues revealed facet-/shape-dependent catalytic activities of single Pd NPs using single FLM.[123] The same group also monitored the temperature-dependent and size-dependent catalytic activities of individual Au nanocatalysts[124] and Au clusters levels,[125] respectively. Due to their unique electronic, mechanical, and structural properties, single-walled carbon nanotubes (SWNTs) have received immense consideration for diverse applications including energy harvesting, catalysis, sensing, and nanoelectronics. The Chen group reported a single molecule FLM to evaluate the electrocatalytic properties of SWNTs.[126] The wide-field imaging enabled multiplexed (real-time) observation of SWNTs electrocatalysis at single-active-site and single-reaction resolution. A fluorogenic reaction was designed by using a two-step electroreduction of resazurin (nonfluorescent molecule).

To observe the electrocatalytic activity by SWNTs at a single molecule level, an indium tin oxide (ITO) working electrode was decorated with individual SWNTs. Under a constant negative potential, resazurin electrochemically reduced to resorufin, leading to stochastic FL bursts. As a result, it was visually confirmed that electrocatalytic reactions occurred at discrete reactive sites (locations), revealing the heterogeneous electronic properties of the individual SWNTs. It was found that the interfacial electron-transfer kinetics are applied and potential dependent between the SWNTs and adsorbed molecules.

Controlling and understanding the gradual decay (stability) of catalysts is crucial for diverse applications, including catalysis, sensing, and nanoscale electronics. The Xu group investigated the in situ deactivation of an individual Pt/C electrocatalyst during hydrogen-oxidation reaction (HOR) at single particle/molecule level by combining the traditional electrochemical method with single molecule FLM.[129] It was found that HOR-induced dissolution or electroetching of PtNPs could lead to Pt/C catalyst activity reduction. The incubation periods and spontaneous regeneration of the activities of Pt electrocatalysts

https://doi.org/10.1021/acsmeasuresciau.3c00052
ACS Meas. Sci. Au 2024, 4, 3–24

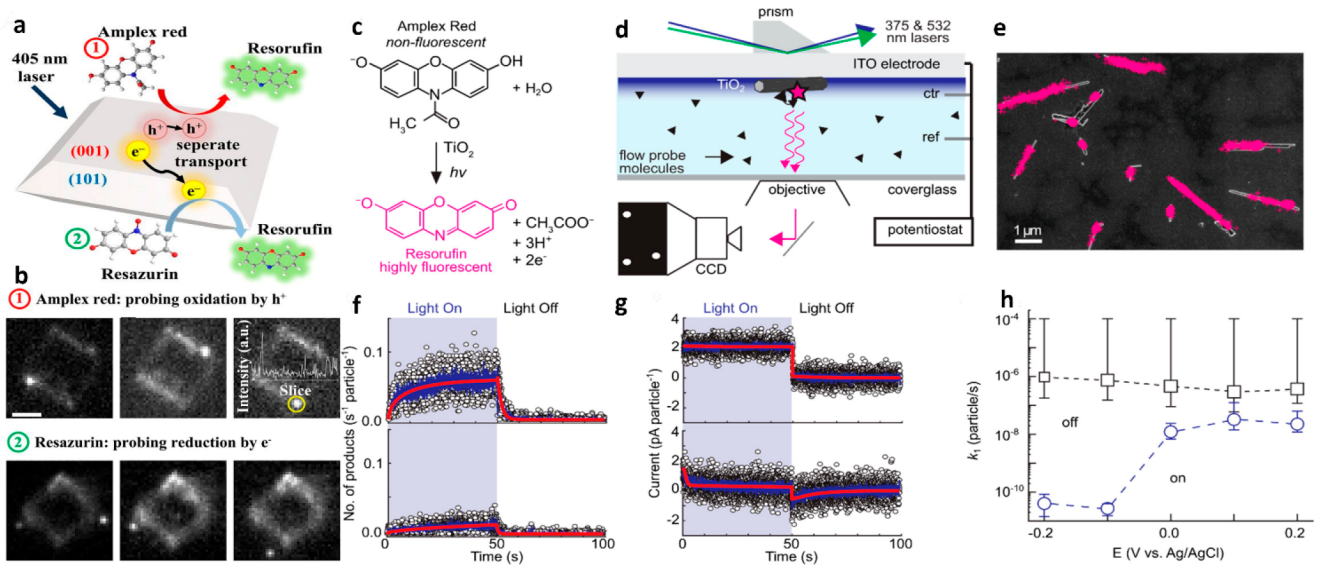

Figure 8. (a) Schematic showing the photocatalytic oxidation and reduction reactions of AR and resazurin on an individual TiO_2 particle, respectively. (b) Single-molecule FL images reveal the photocatalytic oxidation ① of AR and reduction ② of resazurin on a single TiO_2 particle at various times. Inset in ①: Time trace of FL intensity recorded over the yellow-color circled area. Scale bar: 1 μm. Reprinted from ref 134 with permission from the US National Academy of Sciences, copyright 2019. (c) Scheme showing the conversion mechanism of nonfluorescent AR to FL resorufin. (d) TIRFM setup for single-molecule FLM. (e) SEM graphic presenting the TiO_2 NRs onto an ITO surface. Wherein pink color spots symbolize single product molecules. (f, g) Images showing the photoelectrochemical current dynamics and surface reaction intermediates vs electrochemical applied potential. (h) Image plotting the rate constant potential dependence under light Off (black squares) and On (blue circles) intervals. Reprinted with permission from ref 92 with permission from the Electrochemical Society, copyright(2019.

were also monitored at an individual particle level. These insights could be useful for designing high performance catalysts for fuel cells and related energy applications.

Understanding the nanoconfinement effects in catalytic reactions is crucial to designing highly efficient catalysts. Fang and colleagues designed an in situ FLM to reveal single catalytic turnover events on individual PtNPs in nanoconfined environments (Figure 6h).[127] A superlocalization, single-molecule-based imaging approach was utilized under in situ conditions to differentiate and reveal the dynamic catalytic reaction kinetics and heterogeneous molecular transport in the nanopores at single-particle and single-molecule turnover resolution. The results revealed that the rate of reaction was remarkably enhanced in the nanoconfined environment, while reactant molecule adsorption on PtNPs surfaces was weakened because of the limited/restricted molecular adsorption. This work holds great potential to quantitatively understand, evaluate, and differentiate complex nanoconfinement effects and to rationally design high-performance catalysts.

Recently, the Xu and Hyeon groups introduced an electrochemical-single molecule FLM to reveal the kinetics (electron-transfer coefficients and standard rate kinetics etc.) and dynamic heterogeneity (potential dependent) of two-electron oxygen reduction reaction (ORR) on the level of single Fe_3O_4 NPs (Figure 6i).[128] This work provides a detailed study of the electrocatalytic (especially ORR) processes at a single particle/molecule level, which could help in developing better functional (catalytic) materials. In a recent work, Zhao and co-workers reported a dual-mode microscopic method with correlative ECL and vis-absorption imaging of the individual stages of the electrocatalysis with high resolution and speed for in-depth analysis at single electrocatalyst level (Figure 7a).[130] The oxygen evolution catalyzed by $Co(OH)_2$ nanoplates was used as a representative catalyst. This readily applicable method of correlated optical imaging allows in situ mapping of the fast-evolving heterogeneous electrocatalytic process. The information obtained is expected to help in the rational and improved design of electrocatalysts.

5.5. Single Particle Photo(electro)catalysis

Photo(electro)chemical processes have attracted great interest for inexpensive conversion of solar energies to fuels. In a recent example, Zheng group developed a single particle spectroscopy for visualizing the spatially distributed defects on individual particles of $BiVO_4$ by applying PL lifetime mapping (Figure 7b).[131] Likewise, single-particle PL microscopy has been reported for investigating the defects of single Cu_2O microcrystals, revealing their corresponding heterogeneous photocorrosion activity (Figure 7c, d).[132] Understanding the photogenerated hole and electron pair behavior, photocatalytic active sites, and reaction processes on a single particle (catalyst) level is promising for developing efficient catalysts. In particular, titanium oxide (TiO_2) with various morphologies and different crystal structures has been documented as a powerful photocatalyst for diverse catalytic processes due to its high reactivity, nontoxicity, and chemical stability.[133] For example, Majima and colleagues visualized the dynamic photogenerated hole−electron pair behavior and identified the (single-molecule level) photocatalytically active sites on an individual TiO_2 particle by using laser-scanning confocal microscopy and quasi-TIRFM.[134] Two fluorogenic reactions were utilized as probes to investigate photocatalytic redox reactions on a single TiO_2 particle. Photogenerated holes and electrons were probed on a single TiO_2 particle by the oxidation of AR and reduction of resazurin, respectively (Figure 8a). Various FL burst events were detected under 405 and 532 nm laser photoirradiations and their positions were identified by applying centroid analysis. It is found that FL spots were preferentially located on the crystal (particle) edges and corners during both oxidation and reduction processes (Figure 8b).

https://doi.org/10.1021/acsmeasuresciau.3c00052
ACS Meas. Sci. Au 2024, 4, 3−24

Both experimental and density functional theory (DFT) calculations proved that surface defects near edges/corners acted as efficient active (catalytic) sites for the photocatalytic reactions of TiO_2 particles. This work holds great potential for understanding the mechanism of photocatalytic reactions and real-time monitoring of oxidation/reduction processes in heterogeneous catalysis.

By coupling super-resolution technique with wide-field single molecule FLM, Chen group developed a novel approach for optimizing the catalyst-modified photoanodes during the splitting of water.[91] To ensure higher photocatalytic efficiency of photogenerated holes in the water oxidation process, the authors modified the photoanode with an oxygen evolution catalyst to reduce the onset potential and enhance the photocurrent response. A high temporal resolution of ∼15 ms and spatial resolution of ∼30 nm was achieved for mapping the hole- and electron-driven photoelectrocatalytic reactivities (with selective laser irradiation) on an individual TiO_2 NR level. To achieve this target, the authors dispersed single-crystalline rutile TiO_2 NRs onto an ITO surface in a microfluidic photoelectrochemical cell. The photogenerated electron-induced resazurin and photogenerated hole-induced AR solutions were flowed through the cell. The hole-induced reactions happened in a nonuniform manner on individual NRs as the applied potential exceeded − 0.3 V. Particularly, the active sites (hot spots) with higher hole activities exhibited enhanced catalytic activities (most reactions appeared). In a similar fashion, electron-induced reactions appeared in a nonhomogeneous manner below − 0.4 V. This work could reveal a direct correlation between the structure (heterogeneity) and catalytic activity of functional materials.

Although super-resolution FLM has made several breakthroughs in single entity fluorescent imaging, these techniques cannot be used for nonfluorescent species. To solve this challenge, Chen and colleagues introduced a super-resolution competition-enabled imaging technique (COMPEITS) for studying nonfluorescent processes.[90] COMPEITS involved two competing catalytic reactions on an individual (catalyst) particle: a nonfluorescent target reaction and an auxiliary fluorogenic reaction. The nonfluorescent reaction could suppress the fluorogenic reaction rate, leading to a change in fluorescent emission. By applying this strategy, the authors mapped a nonfluorescent surface (photoelectrocatalytic) reaction on a single photocatalyst particle (bismuth vanadate $BiVO_4$) with nanometer precision. A subparticle-level biphasic shape dependence was uncovered, which is crucial for designing catalysts with optimal reactant adsorption efficacy. In this work, an operando approach was developed to provide spatially resolved information on nonfluorescent entities COMPEITS could be applied for interrogating various surface reactions such as heterogeneous catalysis, materials engineering, nanotechnology, and other energy sciences.

Understanding reaction processes at the electrochemical interfaces is significantly important for the development of electrochemical energy conversion systems. In a recent work, Chen group temporally and spatially resolved the water oxidation involved 1-electron reaction intermediates on the surface of an individual TiO_2 NR photoanode using single-molecule FLM.[92] The authors located the 1-electron intermediate concentration (i.e., $(Ti-OH^{\bullet})_s$) through a fluorogenic probe reaction. This reaction turned AR (i.e., nonfluorescent) to fluorescent resorufin (Figure 8c) through photoelectrochemical oxidation.

The ITO electrode was coated with TiO_2 NRs solution to utilize as a working electrode in a TIRFM setup (Figure 8d). A 375 nm laser was applied to excite a thousand TiO_2 NRs during light on/off periods, while a 532 nm laser was applied for continuous excitation of FL products generated on the surface of NRs. The resulting images were collected at the objective and subsequently processed with an EMCCD camera. The product formation was recorded over the surface of TiO_2 NRs, as displayed by the pink dots in Figure 8e. The black data points represented the generated product molecules (Figure 8f) and the current measured from a thousand TiO_2 particles (Figure 8g), respectively. The solid red lines in Figure 8f, g represented the fitting of a kinetic model. Figure 8h showed the rate constant potential dependence of holes transfer (interfacial) toward OH^- (k1) during light off (black squares) and on (blue circles) intervals.

The Wang group reported an in situ FL-labeling approach to monitor single H_2 nanobubbles produced at the surface of individual cadmium sulfide (CdS) NPs.[93] The authors determined the photocatalytic activity of single catalysts by monitoring the nanobubble growth kinetics in an operando imaging manner. Very recently, Tang and colleagues explored the photoelectron-transfer kinetics of a typical heterostructure photocatalyst, TiO_2-tipped CNTs, on an individual particle level by applying a real-time single molecule FLM.[94] This work provides deep insights (theoretical basis) into the photo-electron-transfer processes (kinetics information and behaviors) and guide for designing high performance photocatalysts.

5.6. Single Particle Detection Platforms

Nano/micro fabricated (electro)chemical channels/devices present well controlled geometries/ configurations those can confine reaction volumes to the nano/microscale, enabling highly amplified responses.[135] Importantly, microbeads based ECL systems, nanofluidic devices, and microfabricated BPEs can be applied as highly promising platforms for achieving mechanistic understandings and ultrasensitive detections. The wireless nature of BPE allows control over large electrode arrays with a single power source.[136] For example, Crooks and colleagues designed a large-scale (∼1000 individual gold BPEs) microfabricated array on a glass slide. ECL was generated at the anodic end of each BPE under sufficient driving voltage.[137] This type of massive parallel BPEs arrays could be utilized for a diverse range of screening and sensing applications.[138]

Microfabricated nanodevices with nanoscale confinement of analytes (chemical reaction volume) and precise control over the nanochannel geometry enable highly amplified detection. For instance, the Mathwig and Sojic groups first demonstrated stable generation of ECL emission by ECL in transparent nanofluidic devices by exploiting nanogap amplification.[139] The authors compared ECL annihilation and classic redox cycling through continuous oxidation/reduction of luminophores ($Ru(bpy)_3^{2+}$) at electrodes fixed at the bottom and top of a 100 nm nanochannel. This close vicinity between electrodes leads to fast diffusion, resulting in efficient annihilation reactions (attomole luminophore quantities). Moreover, a short diffusive distance also reduced degradation by contaminants, leading to stable ECL emission under ambient conditions. This type of nanogap transducers can be exploited for developing multicolor ECL systems and investigating pathways in ECL.[139]

In a recent report, the Su group reported a combination of microtube electrodes and ECL microscopy for measuring the thickness of ECL layer and deciphering the reaction

https://doi.org/10.1021/acsmeasuresciau.3c00052
ACS Meas. Sci. Au 2024, 4, 3−24

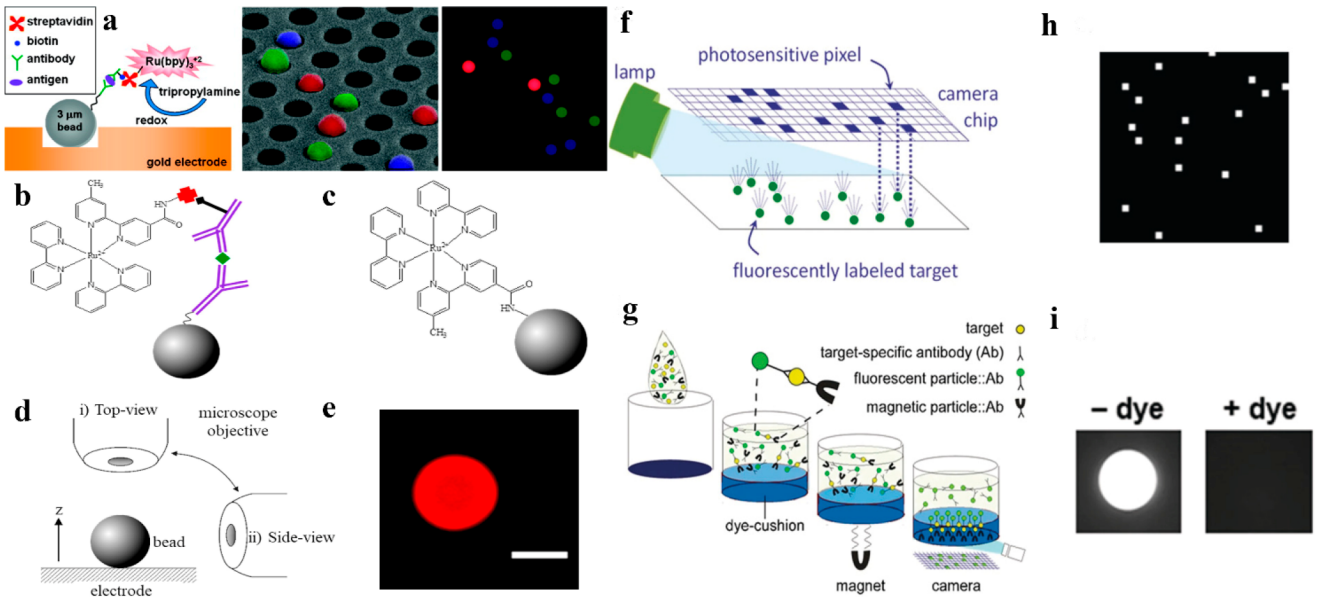

Figure 9. (a) Schematic illustration of a sandwich immunoassay, wherein a bead-based platform was constructed to achieve the ECL detection of multiple antigens simultaneously in a microarray format. Reprinted from ref 141 from American Chemical Society, copyright 2009. (b) Schematic illustration of a sandwich bead-based immunoassay with an ECL readout. (c) Schematic showing the functionalization of a PS bead with an ECL label. (d) Schematic of the two different microscope objective configurations (i.e., top-view and side-view) utilized for imaging the labeled bead. (e) PL image (top view) of a ruthenium (homogeneously distributed) labeled PS bead via a sandwich immunoassay format. The scale bar was 10 μm. Reprinted from ref 142 with permission from Elsevier, copyright 2020. (f) Schematic illustration of the detection/imaging of individual fluorescent beads (bound with molecular targets) on the camera's chip by capturing one or a small group of pixels without the requirement of magnified microscope. (g) After the formation of the immunocomplex, the magnetic beads were drawn toward the microwell bottom (through dye cushion) by applying a magnet and deposited on the imaging surface. Only fluorescent beads in proximity of the surface were excited due to the excitation light absorption (deep into the well). (h) Digital camera recording of fluorescent beads as bright pixels. (i) Images of wells displaying the comparison with and without dye for revealing the effectiveness of the dye-cushion layer. Reprinted from ref 95 with permission from the Springer Nature under a Creative Commons Attribution 4.0 International License.

mechanisms.[140] The use of labeled microbeads is a well-accepted trend for constructing sensitive ECL immunoassays/biosensors. Sojic and Walt groups demonstrated the possibility of conducting multiplexed assays in a microarray format using ECL imaging as a readout mechanism resolved at an individual bead level (Figure 9a).[141] This multiplexed ECL platform was constructed by loading polystyrene (PS) microspheres (3.1 μm) into the electrode wells and modifying their surfaces with three capture antibodies. By exposing antibody-functionalized microbeads to antigen, biotinylated detection antibodies, and $Ru(bpy)_3^{2+}$ streptavidin complex, an EMCCD camera was utilized to individually image each bead emitting ECL to simultaneously detect (targeted) three antigens in the array. This platform could be applied for performing multiplex DNA assays and analyzing dozens of analytes simultaneously.[141]

Better understanding of the mechanistic pathways of ECL generation is crucial for designing highly efficient detection systems with the optimal generation and collection of ECL emission. To tackle this challenge, Sojic and colleagues investigated the ECL mechanism of model system, $Ru(bpy)_3^{2+}$-DBAE or TPrA, by mapping the (3D distribution) ECL reactivities at an individual bead level.[143] The $Ru(bpy)_3^{2+}$-functionalized PS microbeads (diameter $\sim$ 12 μm) were achieved via a peptide bond or *via* a sandwich immunoassay. Reactivity mapping on an individual bead discloses the mechanistic pathway that results in ECL generation. The highest ECL emission was observed in the micrometric region (3 μm distance from the electrode), wherein the concentration of diffusing TPrA radicals (TPrȦ and $TPrA^{+}$) and surface-confined $Ru(bpy)_3^{2+}$ was highest locally. The lifetime of the TPrA-derived radicals (e.g., TP^{+}) was measured by the ECL profiles. In contrast to TPrA, DBAE generated weak ECL emission in the bead-based format, indicating formation of less stable radical intermediates (shorter lifetime). The same group further utilized this concept for investigating heterogeneous ECL bioassays using single $Ru(bpy)_3^{2+}$-decorated PS beads.[142] By mapping the ECL reactivities and PL, the authors disclosed the complex ECL mechanism and key processes leading to decreased ECL emission over time (ECL stability) using TPrA as a model coreactant in heterogeneous bioassays (Figure 9b–e). The 3D (single microbead) imaging platform could be utilized for developing new analytical strategies, revealing the mechanistic pathway in bioassays, and selecting new coreactants with enhanced sensitivity. Later, the same group reported an innovative strategy to tune the ECL-emitting layer ($Ru(bpy)_3^{2+}$-TPrA system) based on chemical lens effects.[144] The change in the concentration of the phosphate buffer (buffer capacity) could alter both the thickness of the ECL-producing area and the rate of ECL reactions. The authors precisely controlled the distribution of the ECL emission through single micrometric bead-based mapping of the ECL reactivity, which allowed mechanistic insights and holds strong potential in ECL microscopy-based bioassays.[144,145]

To enhance the performance of bioassays, diverse types of functional materials have been utilized as immunoassays labels. Particularly, NPs with luminescence characteristics allow the direct visualization (optical readout) of the target analyte at a single molecule level. In comparison to molecular labels, NPs exhibit normally stronger emissions that can enable easier signal detection (readout). For example, the Zhang group used a FL

https://doi.org/10.1021/acsmeasuresciau.3c00052
ACS Meas. Sci. Au 2024, 4, 3–24

imaging method for multiplex detection of three distinct types of single virus (avian influenza) particles by utilizing color-encoded magnetic beads.[146] In another work, Stucky and colleagues embedded distinct colors/ratio upconversion nanocrystals (UPNCs) into polymer microbeads to generate barcodes for multiplexed DNA detection.[147] By using confocal microscopy, labels were detected at a single bead level. The amount and presence of target sequence were identified with traditional fluorescent dyes, while the DNA sequence was detected based on upconversion encoding signals. Gite and colleagues developed a sandwich assay by utilizing (i) a fluorescent microparticle, (ii) a magnetic particle, (iii) *Clostridium difficile*, (iv) anti-*C. difficile* capture and detection antibodies.[95] A mixture of iodixanol (density agent) and a dye-cushion reagent with visible-light-absorbing properties was dried on each microwell bottom part (Figure 9f–i). After the addition of immunoreagents, a magnet was used to pull the magnetic beads toward the bottom part of microplate. Due to the density agent, the dye stayed at the bottom and absorbed all visible light, resulting in significantly reduced background FL of unbound FL particles. As a result, fluorescent beads were recorded with a digital camera chip as bright pixels.

6. CONCLUSIONS AND FUTURE PERSPECTIVES

Single particle imaging/detection is an emerging area of research that has provided a broader understanding of numerous (electro)chemical processes of diverse types of particles, especially at the individual level. The implemented experiments extracted the information about the characteristics of the particles (catalytic ability, confined content, concentration, size distribution, individual size, and so on), as well as the quantified kinetics and qualified mechanisms of the corresponding reactions; charge transfer and mass transfer of impact particles (electron transfer and electron/ion transfer processes). Moreover, coupling computational and machine learning tools with luminescence (optical) microscopies could stimulate breakthrough research for optimizing/designing/simulating next generation energy devices and catalysts.[148−152]

Super-resolution FL and ECL microscopies have been used to reveal the structure−property relationship of single particles by imaging reactants/products and surface reaction hot spots of catalytic reactions at a single molecule/particle level with nanometer precision. Such information could be utilized for designing and developing high performance catalysts. In contrast, super-resolution CL microscopy is still at an emerging stage for imaging/detecting single particles. We have also briefly tabulated the important characteristics of CL, ECL, and PL microscopies (Tables 1 and 2).[35] The rapid improvements in luminescence-based analytical methods and instrumentation hold enormous potential for single-entity analysis. Despite the remarkable success of these techniques, there are still numerous challenges that these techniques are currently facing. Some potential future directions can be briefly written down as follows:

(i) **Theoretical and statistical insights**. The recording of a single particle (single-entity) response with luminescence-based approaches is a significant technical achievement. However, additional attention is required for a better understanding of the relevance of numerous single particle measurements. For example, modeling of measurements, statistical analysis of signals, and comparison of single particle measurement to that of ensemble measurement will be crucial to completely understand the impacts of single particle detection. Therefore, it is crucial to deepen the theoretical and statistical insights into the imaging/detection of single particles, and develop their application in diverse fields, including energy (electrocatalysis, energy storage devices), drug delivery systems (biopharmaceuticals), cata-/biocatalytic materials, and competitively cheap, simple, and fast bio- and environmental sensors.

(ii) **Instrumental advances**. Pushing the limits of CL/ECL instrumentations for single-particle imaging/detection is a significant present challenge. Although the absence of an excitation light source significantly simplifies the experimental operation and instrumentation of CL, which improves the detection sensitivity due to the scattering background elimination. However, it is a challenging task to construct CL-based detection/imaging platform for single particle detection due to direct (chemical reaction) mode of light generation. In contrast, ECL microscopy and FLM-based detection/imaging has made great breakthroughs in single-particle imaging/detection. ECL microscopy can achieve single entity detection up to tens of nanometers (diameter). However, the temporal and spatial resolutions still require further improvements for monitoring (during a chemical reaction) transient processes and recording/imaging fine structure within a NP. Therefore, it is necessary to keep looking for new ways to improve instrumentation, detection principles, setups/ configurations (strategies), and light capturing tools and optical components (e.g., 2D photodetectors, objectives).

(iii) **Preparation of novel electrodes and luminophores**. The preparation of novel electrodes and luminophores are crucial for obtaining a higher electron-transfer rate and higher light emission efficiency, respectively. However, fabrication of nano/microelectrodes and fluidic devices with respectively reproducible morphology and controlled nanochannel geometry are highly challenging. Moreover, the background from diffusion layer of ECL and substrate electrode could affect the measurements. As the single entity emits very weak CL/ECL light, development of new light generating systems (luminophores and coreactants) may significantly enhance the imaging resolution and emission intensity. Recently, near-infrared materials,[153,154] aggregation-induced polymers,[155,156] nanocrystals,[157] and clusters[158] with high luminous efficiency and stability have been documented, which may replace the classically utilized luminol-H_2O_2 and $Ru(bpy)_3^{2+}$-TPrA pairs and subsequently advance single-particle detection. Moreover, the use of nanoluminophores (e.g., doped NPs or QDs), multicolor ECL emission, and combination of ECL with BPEs can promote the development of ECL-microscopy based original applications. In FLM, the quenching effects from local environments and rapid diffusion of fluorescent molecules makes it a challenging task to clearly detect all diffusing fluorophores. Therefore, it is crucial to develop highly stable and brighter fluorescent probes for efficient detections.

(iv) **Chemical amplification schemes/Chen's COMPEITS/ single-molecule labeling**. The utilization of chemical amplification schemes is a recurring theme in single-particle detections, which could get control of instrument

https://doi.org/10.1021/acsmeasuresciau.3c00052
ACS Meas. Sci. Au 2024, 4, 3−24

limitations and SNR. For example, catalytic NP impact studies and single-molecule redox cycling both get benefit from sharp chemical amplification schemes. Such schemes may find diverse applications, such as conversion of signals from ions/electrons to photons using luminescence approaches deliver strong basis to enhance single particle imaging/detections. Moreover, several catalytic reactions do not involve fluorescent species for practical applications, which limit the applicability of FLM. To cross these barriers, new detection strategies including Chen's COMPEITS, and single-molecule labeling have been documented for probing the non-fluorescent processes which could expand the applications of single molecule FLM.[88]

(v) **Imaging individual electrochemical reactions**. Although modern optical approaches can reveal stochastic information about various chemical processes, probing single-molecule solution chemistry remains an arduous task. In a recent breakthrough, Feng group developed a direct ECL-microscopy based method for imaging single photons (visualizing single molecule) produced from individual chemical-reactions (ECL reaction event) in aqueous solutions.[87] Some special strategies were used to detect single reactions. For example, a dilute solution was utilized for ensuring the spatial separation of the molecules and fast cameras were applied to record the rapid ECL reaction events. Because the reactions only occur in proximity or at the electrode surface, this method could directly capture single photons (position) emitted by single excited molecules by imaging the electrode itself or molecules on its surface. By adjusting the reactivity of emitter and coreactant, single ECL reaction event can be isolated in space and time. This method opens numerous opportunities for any reactions involving electron transfer events, investigating individual electrochemical reactions, developing new strategies for (cell) imaging and bioassays, and may get adopted by diverse scientific communities.

(vi) **Real-time detection/imaging**. Real-time detection/imaging using CL and ECL techniques is a significant challenge. Recently, Zhao and co-workers introduced an innovative real-time dual-mode analysis of the OER process on a single nanoplate of cobalt-layered hydroxide.[130] The electrocatalytic process can be imaged in real-time with the ECL emission produced by luminol when oxidized by H_2O_2, an OER byproduct. More research efforts must be focused on developing real-time CL and ECL based approaches by constructing efficient electrodes for ECL and substrates for CL measurements.

(vii) **Improving selectivity**. Selective detection of a specific target is another significant challenge for analytical applications, especially at the level of an individual particle (entity). Different strategies and tricks such as potential waveforms and selective coatings have been successfully utilized for selective detections. Moreover, ion selective electrodes can be utilized for selective discrimination of various ionic species, however, these can suffer with poor temporal resolution. The capability to detect single entity in the presence of potential interfering entities (background) is an important but challenging task in real samples detections. The methods/strategies to improve selectivity may utilize the incorporation of orthogonal techniques or incorporation of biological paradigms.

(viii) **Hybrid approaches**. Hybrid techniques are revolutionizing the single-particle measurements. Optical approaches have rapidly improved in sensitivity, speed, resolution and have extremely wide adoption in recent years. Coupling optical techniques with electrochemical approaches/techniques are bringing several exciting applications in single-particle analysis.[159−162] This area of research is rapidly evolving, and luminescence-based microscopies are being utilized in combination with various other approaches such as dark-field microscopy and electron microscopy for single particle imaging/detection. However, coupling FLM with electron microscopy could only be utilized in ex situ mode, which cannot provide accurate information about component- and structural-dependent reactivity of single catalysts. Therefore, more efforts should be directed toward in situ combing FLM with other techniques, including surface enhanced Raman scattering and high-resolution transmission electron microscopy (TEM), SEM, to real-time probe the electrocatalytic reactions with an atomic resolution. Moreover, multidimensional/multimodal techniques can be used for comprehensive characterization of single particles. It is believed that hybrid techniques will spread the concept of single-particle analysis to various new arenas soon.

Of note, developing powerful luminescence approaches for single particle imaging/detection can identify catalytically active sites, visualize key reaction processes in real-time, clarify the structure−function relationships, elucidate the underlying mechanisms, and improve (bio)analytical (detection/imaging) applications. Beyond method development and technological progress, luminescence-based detection and imaging approaches will continue to provide insightful knowledge in the single-entity detection field and enable exciting opportunities and promising applications in diverse research fields.

AUTHOR INFORMATION

Corresponding Author

Muhammad Saqib − *Institute of Chemistry, Khawaja Fareed University of Engineering and Information Technology, Rahim Yar Khan 64200, Pakistan*; orcid.org/0000-0001-6168-4205; Email: muhammad.saqib@kfueit.edu.pk

Authors

Mariam Zafar − *Institute of Chemistry, Khawaja Fareed University of Engineering and Information Technology, Rahim Yar Khan 64200, Pakistan*

Mohamed Ibrahim Halawa − *Department of Pharmaceutical Analytical Chemistry, Faculty of Pharmacy, Mansoura University, Mansoura 35516, Egypt; Department of Chemistry, College of Science, United Arab Emirates University, Al Ain 15551, United Arab Emirates;* orcid.org/0000-0001-6358-2691

Shahzad Murtaza − *Institute of Chemistry, Khawaja Fareed University of Engineering and Information Technology, Rahim Yar Khan 64200, Pakistan*

Ghulam Mustafa Kamal − *Institute of Chemistry, Khawaja Fareed University of Engineering and Information Technology, Rahim Yar Khan 64200, Pakistan*

https://doi.org/10.1021/acsmeasuresciau.3c00052
ACS Meas. Sci. Au 2024, 4, 3−24

Guobao Xu − *State Key Laboratory of Electroanalytical Chemistry, Changchun Institute of Applied Chemistry, Chinese Academy of Sciences, Changchun, Jilin 130022, China; School of Applied Chemistry and Engineering, University of Science and Technology of China, Hefei 230026, China;* orcid.org/0000-0001-9747-0575

Complete contact information is available at: https://pubs.acs.org/10.1021/acsmeasuresciau.3c00052

Author Contributions

The manuscript was written through contributions of all authors. CRediT: **Muhammad Saqib** conceptualization, funding acquisition, project administration, writing-original draft; **Mariam Zafar** formal analysis, writing-review & editing; **Mohamed Ibrahim Halawa** formal analysis, investigation, visualization; **Shahzad Murtaza** software, validation, writing-review & editing; **Ghulam Mustafa Kamal** visualization, writing-review & editing; **Guobao Xu** resources, supervision, writing-review & editing.

Funding

This work was financially supported by the National Natural Science Foundation of China (Nos: 22150410330, 22174136) and the Ministry of Science and Technology of the People's Republic of China (2023YFE0201800).

Notes

The authors declare no competing financial interest.

■ ACKNOWLEDGMENTS

The authors greatly acknowledge the fruitful discussion with Dr. Rui Hao from Southern University of Science and Technology Shenzhen during the preparation of manuscript. The authors also acknowledge the support from Khwaja Fareed University of Engineering & Information Technology, Rahim Yar Khan Pakistan.

■ REFERENCES

(1) Baker, L. A. Perspective and Prospectus on Single-Entity Electrochemistry. *J. Am. Chem. Soc.* **2018**, *140* (46), 15549−15559.
(2) Wang, W. Imaging the chemical activity of single nanoparticles with optical microscopy. *Chem. Soc. Rev.* **2018**, *47* (7), 2485−2508.
(3) Yang, H.; Saqib, M.; Hao, R. Single-Entity Detection With TEM-Fabricated Nanopores. *Front Chem* **2021**, *9* (305), No. 664820.
(4) Lai, S. C.; Dudin, P. V.; Macpherson, J. V.; Unwin, P. R. Visualizing zeptomole (electro)catalysis at single nanoparticles within an ensemble. *J. Am. Chem. Soc.* **2011**, *133* (28), 10744−7.
(5) Kim, J.; Renault, C.; Nioradze, N.; Arroyo-Curras, N.; Leonard, K. C.; Bard, A. J. Electrocatalytic Activity of Individual Pt Nanoparticles Studied by Nanoscale Scanning Electrochemical Microscopy. *J. Am. Chem. Soc.* **2016**, *138* (27), 8560−8.
(6) Zhou, X.; Andoy, N. M.; Liu, G.; Choudhary, E.; Han, K. S.; Shen, H.; Chen, P. Quantitative super-resolution imaging uncovers reactivity patterns on single nanocatalysts. *Nat. Nanotechnol.* **2012**, *7* (4), 237−41.
(7) Actis, P.; Maalouf, M. M.; Kim, H. J.; Lohith, A.; Vilozny, B.; Seger, R. A.; Pourmand, N. Compartmental genomics in living cells revealed by single-cell nanobiopsy. *ACS Nano* **2014**, *8* (1), 546−53.
(8) Wang, F.; Wen, S.; He, H.; Wang, B.; Zhou, Z.; Shimoni, O.; Jin, D. Microscopic inspection and tracking of single upconversion nanoparticles in living cells. *Light Sci. Appl.* **2018**, *7* (4), 18007.
(9) Fan, F.-R. F.; Park, S.; Zhu, Y.; Ruoff, R. S.; Bard, A. J. Electrogenerated Chemiluminescence of Partially Oxidized Highly Oriented Pyrolytic Graphite Surfaces and of Graphene Oxide Nanoparticles. *J. Am. Chem. Soc.* **2009**, *131* (3), 937−939.
(10) Wilson, A. J.; Devasia, D.; Jain, P. K. Nanoscale optical imaging in chemistry. *Chem. Soc. Rev.* **2020**, *49* (16), 6087−6112.
(11) Žalud, M.; Prysiazhnyi, V.; Bednařík, A.; Preisler, J. Detection of Single Ag Nanoparticles Using Laser Desorption/Ionization Mass Spectrometry. *J. Am. Soc. Mass Spectrom.* **2023**, *34* (7), 1459−1466.
(12) Long, Y. T.; Unwin, P. R.; Baker, L. A. Single-Entity Electrochemistry: Fundamentals and Applications. *ChemElectroChem* **2018**, *5* (20), 2918−2919.
(13) Patrice, F. T.; Qiu, K.; Ying, Y. L.; Long, Y. T. Single Nanoparticle Electrochemistry. *Annu. Rev. Anal. Chem.* **2019**, *12* (1), 347−370.
(14) Clausmeyer, J.; Schuhmann, W. Nanoelectrodes: Applications in electrocatalysis, single-cell analysis and high-resolution electrochemical imaging. *Trac-Trend. Anal. Chem.* **2016**, *79*, 46−59.
(15) Noël, J.-M.; Lemineur, J.-F. Optical microscopy to study single nanoparticles electrochemistry: From reaction to motion. *Curr. Opin. Electrochem.* **2021**, *25*, No. 100647.
(16) Wang, Y.; Shan, X.; Tao, N. Emerging tools for studying single entity electrochemistry. *Faraday Discuss.* **2016**, *193* (0), 9−39.
(17) Bentley, C. L.; Kang, M.; Unwin, P. R. Nanoscale Surface Structure-Activity in Electrochemistry and Electrocatalysis. *J. Am. Chem. Soc.* **2019**, *141* (6), 2179−2193.
(18) Saqib, M.; Fan, Y.; Hao, R.; Zhang, B. Optical imaging of nanoscale electrochemical interfaces in energy applications. *Nano Energy* **2021**, *90*, No. 106539.
(19) Wang, Y.; Cao, Z.; Yang, Q.; Guo, W.; Su, B. Optical methods for studying local electrochemical reactions with spatial resolution: A critical review. *Anal. Chim. Acta* **2019**, *1074*, 1−15.
(20) Bouffier, L.; Doneux, T. Coupling electrochemistry with in situ fluorescence (confocal) microscopy. *Curr. Opin. Electrochem.* **2017**, *6* (1), 31−37.
(21) Brasiliense, V.; Berto, P.; Combellas, C.; Tessier, G.; Kanoufi, F. Electrochemistry of Single Nanodomains Revealed by Three-Dimensional Holographic Microscopy. *Acc. Chem. Res.* **2016**, *49* (9), 2049−57.
(22) Jiang, D.; Jiang, Y.; Li, Z.; Liu, T.; Wo, X.; Fang, Y.; Tao, N.; Wang, W.; Chen, H. Y. Optical Imaging of Phase Transition and Li-Ion Diffusion Kinetics of Single LiCoO(2) Nanoparticles During Electrochemical Cycling. *J. Am. Chem. Soc.* **2017**, *139* (1), 186−192.
(23) Miao, W. Electrogenerated chemiluminescence and its biorelated applications. *Chem. Rev.* **2008**, *108* (7), 2506−53.
(24) Meng, C.; Knežević, S.; Du, F.; Guan, Y.; Kanoufi, F.; Sojic, N.; Xu, G. Recent advances in electrochemiluminescence imaging analysis. *eScience* **2022**, *2* (6), 591−605.
(25) Liu, Z.; Qi, W.; Xu, G. Recent advances in electrochemiluminescence. *Chem. Soc. Rev.* **2015**, *44* (10), 3117−42.
(26) Kong, W.; Li, Q.; Wang, W.; Zhao, X.; Jiang, S.; Zheng, T.; Zhang, Q.; Shen, W.; Cui, H. Rational design of functional materials guided by single particle chemiluminescence imaging. *Chem. Sci.* **2019**, *10* (21), 5444−5451.
(27) Zhang, J.; Arbault, S.; Sojic, N.; Jiang, D. Electrochemiluminescence Imaging for Bioanalysis. *Annu. Rev. Anal. Chem.* **2019**, *12* (1), 275−295.
(28) Li, L.; Chen, Y.; Zhu, J. J. Recent Advances in Electrochemiluminescence Analysis. *Anal. Chem.* **2017**, *89* (1), 358−371.
(29) Yang, M.; Huang, J.; Fan, J.; Du, J.; Pu, K.; Peng, X. Chemiluminescence for bioimaging and therapeutics: recent advances and challenges. *Chem. Soc. Rev.* **2020**, *49* (19), 6800−6815.
(30) Saqib, M.; Bashir, S.; Li, H.; Wang, S.; Jin, Y. Lucigenin-Tris(2-carboxyethyl)phosphine Chemiluminescence for Selective and Sensitive Detection of TCEP, Superoxide Dismutase, Mercury(II), and Dopamine. *Anal. Chem.* **2019**, *91* (4), 3070−3077.
(31) Saqib, M.; Bashir, S.; Li, H.; Li, C.; Wang, S.; Jin, Y. Efficient Electrogenerated Chemiluminescence of Tris(2,2′-bipyridine)-ruthenium(II) with N-Hydroxysulfosuccinimide as a Coreactant for Selective and Sensitive Detection of l-Proline and Mercury(II). *Anal. Chem.* **2019**, *91* (19), 12517−12524.
(32) Barlow, S. T.; Figueroa, B.; Fu, D.; Zhang, B. Membrane Tension Modifies Redox Loading and Release in Single Liposome Electroanalysis. *Anal. Chem.* **2021**, *93* (8), 3876−3882.

(33) Ben Trad, F.; Wieczny, V.; Delacotte, J.; Morel, M.; Guille-Collignon, M.; Arbault, S.; Lemaître, F.; Sojic, N.; Labbé, E.; Buriez, O. Dynamic Electrochemiluminescence Imaging of Single Giant Liposome Opening at Polarized Electrodes. *Anal. Chem.* **2022**, *94* (3), 1686−1696.
(34) Ma, C.; Cao, Y.; Gou, X.; Zhu, J. J. Recent Progress in Electrochemiluminescence Sensing and Imaging. *Anal. Chem.* **2020**, *92* (1), 431−454.
(35) Zanut, A.; Fiorani, A.; Rebeccani, S.; Kesarkar, S.; Valenti, G. Electrochemiluminescence as emerging microscopy techniques. *Anal. Bioanal. Chem.* **2019**, *411* (19), 4375−4382.
(36) Gou, X.; Xing, Z.; Ma, C.; Zhu, J.-J. A Close Look at Mechanism, Application, and Opportunities of Electrochemiluminescence Microscopy. *Chemical & Biomedical Imaging* **2023**, *1* (5), 414−433.
(37) Ding, H.; Guo, W.; Su, B. Electrochemiluminescence Single-Cell Analysis: Intensity- and Imaging-Based Methods. *ChemPlusChem* **2020**, *85* (4), 725−733.
(38) Creton, R.; Jaffe, L. F. Chemiluminescence microscopy as a tool in biomedical research. *BioTechniques* **2001**, *31* (5), 1098−1105.
(39) Lippert, A. R. Unlocking the Potential of Chemiluminescence Imaging. *ACS Cent. Sci.* **2017**, *3* (4), 269−271.
(40) Wei, Y.; Zhang, Y.; Pan, J.; Chen, T.; Xing, X.; Zhang, W.; Lu, Z. Plasmon-Enhanced Electrochemiluminescence at the Single-Nanoparticle Level. *Angew. Chem., Int. Ed.* **2023**, *62* (2), No. e202214103.
(41) Hu, X.; Yu, S.; Wang, C.; Zhang, X.; Pan, J.; Ju, H. Electrochemiluminescence Imaging at a Single Nanoparticle Scale to Elucidate Diffusion-Accelerated Charge Transfer and Monitor Cell Permeability. *Anal. Chem.* **2023**, *95* (9), 4496−4502.
(42) Xiao, Y.; Xu, W. Single-molecule fluorescence imaging for probing nanocatalytic process. *Chem* **2023**, *9* (1), 16−28.
(43) Chen, P.; Zhou, X.; Shen, H.; Andoy, N. M.; Choudhary, E.; Han, K. S.; Liu, G.; Meng, W. Single-molecule fluorescence imaging of nanocatalytic processes. *Chem. Soc. Rev.* **2010**, *39* (12), 4560−70.
(44) Hao, R.; Peng, Z.; Zhang, B. Single-Molecule Fluorescence Microscopy for Probing the Electrochemical Interface. *ACS Omega* **2020**, *5* (1), 89−97.
(45) Li, W.; Kaminski Schierle, G. S.; Lei, B.; Liu, Y.; Kaminski, C. F. Fluorescent Nanoparticles for Super-Resolution Imaging. *Chemical Reviews* **2022**, *122* (15), 12495−12543.
(46) Chen, M. M.; Zhao, W.; Zhu, M. J.; Li, X. L.; Xu, C. H.; Chen, H. Y.; Xu, J. J. Spatiotemporal imaging of electrocatalytic activity on single 2D gold nanoplates via electrogenerated chemiluminescence microscopy. *Chem. Sci.* **2019**, *10* (15), 4141−4147.
(47) von Diezmann, L.; Shechtman, Y.; Moerner, W. E. Three-Dimensional Localization of Single Molecules for Super-Resolution Imaging and Single-Particle Tracking. *Chem. Rev.* **2017**, *117* (11), 7244−7275.
(48) Zhu, M. J.; Pan, J. B.; Wu, Z. Q.; Gao, X. Y.; Zhao, W.; Xia, X. H.; Xu, J. J.; Chen, H. Y. Electrogenerated Chemiluminescence Imaging of Electrocatalysis at a Single Au-Pt Janus Nanoparticle. *Angew. Chem., Int. Ed.* **2018**, *57* (15), 4010−4014.
(49) Li, F.; Guo, L.; Li, Z.; He, J.; Cui, H. Temporal-Spatial-Color Multiresolved Chemiluminescence Imaging for Multiplex Immunoassays Using a Smartphone Coupled with Microfluidic Chip. *Anal. Chem.* **2020**, *92* (10), 6827−6831.
(50) Wang, R.; Yue, N.; Fan, A. Nanomaterial-enhanced chemiluminescence reactions and their applications. *Analyst* **2020**, *145* (23), 7488−7510.
(51) Su, Y.; Song, H.; Lv, Y. Recent advances in chemiluminescence for reactive oxygen species sensing and imaging analysis. *Microchem. J.* **2019**, *146*, 83−97.
(52) Saqib, M.; Lou, B.; Halawa, M. I.; Kitte, S. A.; Liu, Z.; Xu, G. Chemiluminescence of Lucigenin-Allantoin and Its Application for the Detection of Allantoin. *Anal. Chem.* **2017**, *89* (3), 1863−1869.
(53) Saqib, M.; Gao, W.; Lai, J.; Qi, L.; Majeed, S.; Gilani, M. R.; Xu, G. Hydroxylamine-O-sulfonic acid as an efficient coreactant for luminol chemiluminescence for selective and sensitive detection. *Chem. Commun.* **2015**, *51* (30), 6536−9.
(54) Shah, S. N.; Lin, J. M. Recent advances in chemiluminescence based on carbonaceous dots. *Adv. Colloid Interface Sci.* **2017**, *241*, 24−36.
(55) Saqib, M.; Li, S.; Gao, W.; Majeed, S.; Qi, L.; Liu, Z.; Xu, G. N-Hydroxysuccinimide as an effective chemiluminescence coreactant for highly selective and sensitive detection. *Anal. Bioanal. Chem.* **2016**, *408* (30), 8851−8857.
(56) Yu, D.; Wang, P.; Zhao, Y.; Fan, A. Iodophenol blue-enhanced luminol chemiluminescence and its application to hydrogen peroxide and glucose detection. *Talanta* **2016**, *146*, 655−61.
(57) Borrego-Sanchez, A.; Giussani, A.; Rubio, M.; Roca-Sanjuan, D. On the chemiluminescence emission of luminol: protic and aprotic solvents and encapsulation to improve the properties in aqueous solution. *Phys. Chem. Chem. Phys.* **2020**, *22* (47), 27617−27625.
(58) Saqib, M.; Qi, L.; Hui, P.; Nsabimana, A.; Halawa, M. I.; Zhang, W.; Xu, G. Development of luminol-N-hydroxyphthalimide chemiluminescence system for highly selective and sensitive detection of superoxide dismutase, uric acid and Co(2). *Biosens. Bioelectron.* **2018**, *99*, 519−524.
(59) Roda, A.; Cui, H.; Lu, C. Highlights of analytical chemical luminescence and cataluminescence. *Anal. Bioanal. Chem.* **2016**, *408* (30), 8727−8729.
(60) Tiwari, A.; Dhoble, S. J. Recent advances and developments on integrating nanotechnology with chemiluminescence assays. *Talanta* **2018**, *180*, 1−11.
(61) Bouffier, L.; Sojic, N. Introduction and Overview of Electrogenerated Chemiluminescence. In *Analytical Electrogenerated Chemiluminescence*; The Royal Society of Chemistry: 2019; Chapter 1, pp 1-28.
(62) Zanut, A.; Fiorani, A.; Canola, S.; Saito, T.; Ziebart, N.; Rapino, S.; Rebeccani, S.; Barbon, A.; Irie, T.; Josel, H. P.; Negri, F.; Marcaccio, M.; Windfuhr, M.; Imai, K.; Valenti, G.; Paolucci, F. Insights into the mechanism of coreactant electrochemiluminescence facilitating enhanced bioanalytical performance. *Nat. Commun.* **2020**, *11* (1), 2668.
(63) Saqib, M.; Bashir, S.; Ali, S.; Hao, R. Highly selective and sensitive detection of mercury (II) and dopamine based on the efficient electrochemiluminescence of Ru(bpy)32+ with acridine orange as a coreactant. *J. Electroanal. Chem.* **2022**, *906*, No. 115896.
(64) Richter, M. M. Electrochemiluminescence (ECL). *Chem. Rev.* **2004**, *104* (6), 3003−36.
(65) Saqib, M.; Bashir, S.; Kitte, S. A.; Li, H.; Jin, Y. Acridine orange as a coreactant for efficient electrogenerated chemiluminescence of tris(2,2′-bipyridine)ruthenium(ii) and its use in selective and sensitive detection of thiourea. *Chem. Commun.* **2020**, *56* (38), 5154−5157.
(66) Irkham; Watanabe, T.; Fiorani, A.; Valenti, G.; Paolucci, F.; Einaga, Y. Co-reactant-on-Demand ECL: Electrogenerated Chemiluminescence by the in Situ Production of S2O8(2-) at Boron-Doped Diamond Electrodes. *J. Am. Chem. Soc.* **2016**, *138* (48), 15636−15641.
(67) Chang, M.-M.; Saji, T.; Bard, A. J. Electrogenerated chemiluminescence. 30. Electrochemical oxidation of oxalate ion in the presence of luminescers in acetonitrile solutions. *J. Am. Chem. Soc.* **1977**, *99* (16), 5399−5403.
(68) Leland, J. K.; Powell, M. J. Electrogenerated Chemiluminescence: An Oxidative-Reduction Type ECL Reaction Sequence Using Tripropyl Amine. *J. Electrochem. Soc.* **1990**, *137* (10), 3127−3131.
(69) Miao, W.; Choi, J. P.; Bard, A. J. Electrogenerated chemiluminescence 69: the tris(2,2′-bipyridine)ruthenium(II), (Ru(bpy)3(2+))/tri-n-propylamine (TPrA) system revisited-a new route involving TPrA*+ cation radicals. *J. Am. Chem. Soc.* **2002**, *124* (48), 14478−85.
(70) White, H. S.; Bard, A. J. Electrogenerated chemiluminescence. 41. Electrogenerated chemiluminescence and chemiluminescence of the Ru(2,21 - bpy)32+-S2O82- system in acetonitrile-water solutions. *J. Am. Chem. Soc.* **1982**, *104* (25), 6891−6895.
(71) Xu, G.; Dong, S. Electrochemiluminescence of the Ru(bpy)32+/S2O82- System in Purely Aqueous Solution at Carbon Paste Electrode. *Electroanalysis* **2000**, *12* (8), 583−587.
(72) Lakowicz, J. R. *Principles of Fluorescence Spectroscopy*; Springer: 2013.

(73) Shashkova, S.; Leake, M. C. Single-molecule fluorescence microscopy review: shedding new light on old problems. *Biosci. Rep.* **2017**, *37* (4), No. BSR20170031.
(74) Zhao, W.; Chen, H. Y.; Xu, J. J. Electrogenerated chemiluminescence detection of single entities. *Chem. Sci.* **2021**, *12* (16), 5720−5736.
(75) Voci, S.; Goudeau, B.; Valenti, G.; Lesch, A.; Jovic, M.; Rapino, S.; Paolucci, F.; Arbault, S.; Sojic, N. Surface-Confined Electrochemiluminescence Microscopy of Cell Membranes. *J. Am. Chem. Soc.* **2018**, *140* (44), 14753−14760.
(76) Chen, Y.; Zhao, D.; Fu, J.; Gou, X.; Jiang, D.; Dong, H.; Zhu, J. J. In Situ Imaging Facet-Induced Spatial Heterogeneity of Electrocatalytic Reaction Activity at the Subparticle Level via Electrochemiluminescence Microscopy. *Anal. Chem.* **2019**, *91* (10), 6829−6835.
(77) Fan, Y.; Hao, R.; Han, C.; Zhang, B. Counting Single Redox Molecules in a Nanoscale Electrochemical Cell. *Anal. Chem.* **2018**, *90* (23), 13837−13841.
(78) Moerner, W. E.; Fromm, D. P. Methods of single-molecule fluorescence spectroscopy and microscopy. *Rev. Sci. Instrum.* **2003**, *74* (8), 3597−3619.
(79) Ye, X.; Saqib, M.; Mao, J.; Li, G.; Hao, R. Spatiotemporally super-resolved dendrites nucleation and early-stage growth dynamics in Zinc-ion batteries. *Cell Rep. Phys. Sci.* **2021**, *2* (5), No. 100420.
(80) Chen, M. M.; Xu, C. H.; Zhao, W.; Chen, H. Y.; Xu, J. J. Super-Resolution Electrogenerated Chemiluminescence Microscopy for Single-Nanocatalyst Imaging. *J. Am. Chem. Soc.* **2021**, *143* (44), 18511−18518.
(81) Salinas, G.; Dauphin, A. L.; Voci, S.; Bouffier, L.; Sojic, N.; Kuhn, A. Asymmetry controlled dynamic behavior of autonomous chemiluminescent Janus microswimmers. *Chem. Sci.* **2020**, *11* (28), 7438−7443.
(82) Dauphin, A. L.; Akchach, A.; Voci, S.; Kuhn, A.; Xu, G.; Bouffier, L.; Sojic, N. Tracking Magnetic Rotating Objects by Bipolar Electrochemiluminescence. *J. Phys. Chem. Lett.* **2019**, *10* (18), 5318−5324.
(83) Guo, W.; Ding, H.; Zhou, P.; Wang, Y.; Su, B. Electrochemiluminescence Waveguide in Single Crystalline Molecular Wires. *Angew. Chem., Int. Ed.* **2020**, *59* (17), 6745−6749.
(84) Ma, C.; Wei, H. F.; Wang, M. X.; Wu, S.; Chang, Y. C.; Zhang, J.; Jiang, L. P.; Zhu, W.; Chen, Z.; Lin, Y. Hydrogen Evolution Reaction Monitored by Electrochemiluminescence Blinking at Single-Nanoparticle Level. *Nano. Lett.* **2020**, *20* (7), 5008−5016.
(85) Ma, C.; Wu, W.; Li, L.; Wu, S.; Zhang, J.; Chen, Z.; Zhu, J. J. Dynamically imaging collision electrochemistry of single electrochemiluminescence nano-emitters. *Chem. Sci.* **2018**, *9* (29), 6167−6175.
(86) Zhu, H.; Jiang, D.; Zhu, J. J. High-resolution imaging of catalytic activity of a single graphene sheet using electrochemiluminescence microscopy. *Chem. Sci.* **2021**, *12* (13), 4794−4799.
(87) Dong, J.; Lu, Y.; Xu, Y.; Chen, F.; Yang, J.; Chen, Y.; Feng, J. Direct imaging of single-molecule electrochemical reactions in solution. *Nature* **2021**, *596* (7871), 244−249.
(88) Xiao, Y.; Xu, W. Single-Molecule Fluorescence Imaging of Nanocatalysis. *Chin. J. Chem.* **2021**, *39* (6), 1459−1470.
(89) Hao, R.; Fan, Y.; Zhang, B. Imaging Dynamic Collision and Oxidation of Single Silver Nanoparticles at the Electrode/Solution Interface. *J. Am. Chem. Soc.* **2017**, *139* (35), 12274−12282.
(90) Mao, X.; Liu, C.; Hesari, M.; Zou, N.; Chen, P. Super-resolution imaging of non-fluorescent reactions via competition. *Nat. Chem.* **2019**, *11* (8), 687−694.
(91) Sambur, J. B.; Chen, T. Y.; Choudhary, E.; Chen, G.; Nissen, E. J.; Thomas, E. M.; Zou, N.; Chen, P. Sub-particle reaction and photocurrent mapping to optimize catalyst-modified photoanodes. *Nature* **2016**, *530* (7588), 77−80.
(92) Sambur, J. B.; Shepherd, D. P.; Hesari, M.; Van Erdewyk, M.; Choudhary, E.; Chen, P. Correlated Single-Molecule Reaction Imaging and Photocurrent Measurements Reveal Underlying Rate Processes in Photoelectrochemical Water Splitting. *J. Electrochem. Soc.* **2019**, *166* (5), H3286−H3293.
(93) Su, H.; Fang, Y.; Chen, F.; Wang, W. Monitoring the dynamic photocatalytic activity of single CdS nanoparticles by lighting up H2 nanobubbles with fluorescent dyes. *Chem. Sci.* **2018**, *9* (6), 1448−1453.
(94) An, J. H.; Song, X. T.; Wan, W. B.; Chen, Y. Z.; Si, H. B.; Duan, H. C. A.; Li, L.; Tang, B. Kinetics of the Photoelectron-Transfer Process Characterized by Real-Time Single-Molecule Fluorescence Imaging on Individual Photocatalyst Particles. *ACS Catal.* **2021**, *11* (12), 6872−6882.
(95) Gite, S.; Archambault, D.; Cappillino, M. P.; Cunha, D.; Dorich, V.; Shatova, T.; Tempesta, A.; Walsh, B.; Walsh, J. A.; Williams, A.; Kirby, J. E.; Bowers, J.; Straus, D. A Rapid, Accurate, Single Molecule Counting Method Detects Clostridium difficile Toxin B in Stool Samples. *Sci. Rep.* **2018**, *8* (1), 8364.
(96) Chang, Y. L.; Palacios, R. E.; Fan, F. R.; Bard, A. J.; Barbara, P. F. Electrogenerated chemiluminescence of single conjugated polymer nanoparticles. *J. Am. Chem. Soc.* **2008**, *130* (28), 8906−7.
(97) Pan, S.; Liu, J.; Hill, C. M. Observation of Local Redox Events at Individual Au Nanoparticles Using Electrogenerated Chemiluminescence Microscopy. *J. Phys. Chem. C* **2015**, *119* (48), 27095−27103.
(98) Wilson, A. J.; Marchuk, K.; Willets, K. A. Imaging Electrogenerated Chemiluminescence at Single Gold Nanowire Electrodes. *Nano. Lett.* **2015**, *15* (9), 6110−5.
(99) María-Hormigos, R.; Escarpa, A.; Goudeau, B.; Ravaine, V.; Perro, A.; Kuhn, A. Oscillatory Light-Emitting Biopolymer Based Janus Microswimmers. *Adv. Mater. Interfaces* **2020**, *7* (10), No. 1902094.
(100) Sentic, M.; Loget, G.; Manojlovic, D.; Kuhn, A.; Sojic, N. Light-emitting electrochemical ″swimmers. *Angew. Chem., Int. Ed.* **2012**, *51* (45), 11284−8.
(101) Sentic, M.; Arbault, S.; Goudeau, B.; Manojlovic, D.; Kuhn, A.; Bouffier, L.; Sojic, N. Electrochemiluminescent swimmers for dynamic enzymatic sensing. *Chem. Commun.* **2014**, *50* (71), 10202−5.
(102) Sentic, M.; Arbault, S.; Bouffier, L.; Manojlovic, D.; Kuhn, A.; Sojic, N. 3D electrogenerated chemiluminescence: from surface-confined reactions to bulk emission. *Chem. Sci.* **2015**, *6* (8), 4433−4437.
(103) de Poulpiquet, A.; Diez-Buitrago, B.; Dumont Milutinovic, M.; Sentic, M.; Arbault, S.; Bouffier, L.; Kuhn, A.; Sojic, N. Dual Enzymatic Detection by Bulk Electrogenerated Chemiluminescence. *Anal. Chem.* **2016**, *88* (12), 6585−92.
(104) Dupont, A.; Lamb, D. C. Nanoscale three-dimensional single particle tracking. *Nanoscale* **2011**, *3* (11), 4532−41.
(105) Du, K.; Liddle, J. A.; Berglund, A. J. Three-dimensional real-time tracking of nanoparticles at an oil-water interface. *Langmuir: the ACS journal of surfaces and colloids* **2012**, *28* (25), 9181−8.
(106) Wells, N. P.; Lessard, G. A.; Werner, J. H. Confocal, three-dimensional tracking of individual quantum dots in high-background environments. *Anal. Chem.* **2008**, *80* (24), 9830−4.
(107) Cang, H.; Wong, C. M.; Xu, C. S.; Rizvi, A. H.; Yang, H. Confocal three dimensional tracking of a single nanoparticle with concurrent spectroscopic readouts. *Appl. Phys. Lett.* **2006**, *88* (22), No. 223901.
(108) Hou, S.; Exell, J.; Welsher, K. Real-time 3D single molecule tracking. *Nat. Commun.* **2020**, *11* (1), 3607.
(109) Dick, J. E.; Renault, C.; Kim, B. K.; Bard, A. J. Simultaneous detection of single attoliter droplet collisions by electrochemical and electrogenerated chemiluminescent responses. *Angew. Chem., Int. Ed.* **2014**, *53* (44), 11859−62.
(110) Kim, B. K.; Boika, A.; Kim, J.; Dick, J. E.; Bard, A. J. Characterizing emulsions by observation of single droplet collisions–attoliter electrochemical reactors. *J. Am. Chem. Soc.* **2014**, *136* (13), 4849−52.
(111) Dick, J. E.; Lebegue, E.; Strawsine, L. M.; Bard, A. J. Millisecond Coulometry via Zeptoliter Droplet Collisions on an Ultramicroelectrode. *Electroanalysis* **2016**, *28* (10), 2320−2326.
(112) Fan, F. R.; Bard, A. J. Observing single nanoparticle collisions by electrogenerated chemiluminescence amplification. *Nano. Lett.* **2008**, *8* (6), 1746−9.

(113) Glasscott, M. W.; Dick, J. E. Visualizing Phase Boundaries with Electrogenerated Chemiluminescence. *J. Phys. Chem. Lett.* **2020**, *11* (12), 4803−4808.
(114) Peng, Y. Y.; Qian, R. C.; Hafez, M. E.; Long, Y. T. Stochastic Collision Nanoelectrochemistry: A Review of Recent Developments. *Chemelectrochem* **2017**, *4* (5), 977−985.
(115) Hafez, M. E.; Ma, H.; Peng, Y. Y.; Ma, W.; Long, Y. T. Correlated Anodic-Cathodic Nanocollision Events Reveal Redox Behaviors of Single Silver Nanoparticles. *J. Phys. Chem. Lett.* **2019**, *10* (12), 3276−3281.
(116) Hill, C. M.; Bennett, R.; Zhou, C.; Street, S.; Zheng, J.; Pan, S. Single Ag Nanoparticle Spectroelectrochemistry via Dark-Field Scattering and Fluorescence Microscopies. *J. Phys. Chem. C* **2015**, *119* (12), 6760−6768.
(117) Zhang, F.; Defnet, P. A.; Fan, Y. S.; Hao, R.; Zhang, B. Transient Electrocatalytic Water Oxidation in Single-Nanoparticle Collision. *J. Phys. Chem. C* **2018**, *122* (11), 6447−6455.
(118) Cao, J.; Zhang, D.; Xu, W. Recent progress in single-molecule fluorescence technology in nanocatalysis. *Nano Research* **2022**, *15* (12), 10316−10327.
(119) Chen, M. M.; Xu, C. H.; Zhao, W.; Chen, H. Y.; Xu, J. J. Observing the structure-dependent electrocatalytic activity of bimetallic Pd-Au nanorods at the single-particle level. *Chem. Commun.* **2020**, *56* (23), 3413−3416.
(120) Chen, Y.; Fu, J.; Cui, C.; Jiang, D.; Chen, Z.; Chen, H. Y.; Zhu, J. J. In Situ Visualization of Electrocatalytic Reaction Activity at Quantum Dots for Water Oxidation. *Anal. Chem.* **2018**, *90* (14), 8635−8641.
(121) Dunn, C. B.; Valdez, S.; Qiang, Z. Single-molecule fluorescence microscopy for imaging chemical reactions: Recent progress and future opportunities for advancing polymer systems. *J. Polym. Sci.* **2023**, DOI: 10.1002/pol.20230621.
(122) Shen, M.; Rackers, W. H.; Sadtler, B. Getting the Most Out of Fluorogenic Probes: Challenges and Opportunities in Using Single-Molecule Fluorescence to Image Electro- and Photocatalysis. *Chem. Biomed. Imaging* **2023**, DOI: 10.1021/cbmi.3c00075.
(123) Chen, T.; Chen, S.; Song, P.; Zhang, Y. W.; Su, H. Y.; Xu, W. L.; Zeng, J. Single-Molecule Nanocatalysis Reveals Facet-Dependent Catalytic Kinetics and Dynamics of Pallidium Nanoparticles. *ACS Catal.* **2017**, *7* (4), 2967−2972.
(124) Chen, T.; Zhang, Y.; Xu, W. Single-Molecule Nanocatalysis Reveals Catalytic Activation Energy of Single Nanocatalysts. *J. Am. Chem. Soc.* **2016**, *138* (38), 12414−21.
(125) Zhang, Y.; Song, P.; Chen, T.; Liu, X.; Chen, T.; Wu, Z.; Wang, Y.; Xie, J.; Xu, W. Unique size-dependent nanocatalysis revealed at the single atomically precise gold cluster level. *Proc. Natl. Acad. Sci. USA* **2018**, *115* (42), 10588−10593.
(126) Xu, W.; Shen, H.; Kim, Y. J.; Zhou, X.; Liu, G.; Park, J.; Chen, P. Single-molecule electrocatalysis by single-walled carbon nanotubes. *Nano Lett.* **2009**, *9* (12), 3968−73.
(127) Dong, B.; Pei, Y.; Zhao, F.; Goh, T. W.; Qi, Z.; Xiao, C.; Chen, K.; Huang, W.; Fang, N. In situ quantitative single-molecule study of dynamic catalytic processes in nanoconfinement. *Nat. Catal.* **2018**, *1* (2), 135−140.
(128) Xiao, Y.; Hong, J.; Wang, X.; Chen, T.; Hyeon, T.; Xu, W. Revealing Kinetics of Two-Electron Oxygen Reduction Reaction at Single-Molecule Level. *J. Am. Chem. Soc.* **2020**, *142* (30), 13201−13209.
(129) Zhang, Y.; Chen, T.; Alia, S.; Pivovar, B. S.; Xu, W. Single-Molecule Nanocatalysis Shows In Situ Deactivation of Pt/C Electrocatalysts during the Hydrogen-Oxidation Reaction. *Angew. Chem., Int. Ed.* **2016**, *55* (9), 3086−90.
(130) Zhao, X.; Li, Y.; Cui, Y.; Saqib, M.; Zhang, X.; Hao, R.; Zheng, Z. Spatiotemporally and Chemically Resolved Imaging of Electrocatalytic Oxygen Evolution on Single Nanoplates of Cobalt-Layered Hydroxide. *J. Am. Chem. Soc.* **2023**, *145* (38), 20897−20906.
(131) Zhang, Y.; Liu, Y.; Zhang, T.; Gong, X.; Wang, Z.; Liu, Y.; Wang, P.; Cheng, H.; Dai, Y.; Huang, B.; Zheng, Z. In Situ Monitoring of the Spatial Distribution of Oxygen Vacancies and Enhanced Photocatalytic Performance at the Single-Particle Level. *Nano Lett.* **2023**, *23* (4), 1244−1251.
(132) Lee, J.-K.; Wu, S.; Lim, P. C.; Zhang, Z. Spectrally Resolved Single Particle Photoluminescence Microscopy Reveals Heterogeneous Photocorrosion Activity of Cuprous Oxide Microcrystals. *Nano Lett.* **2022**, *22* (12), 4654−4660.
(133) Li, C.; Koenigsmann, C.; Ding, W.; Rudshteyn, B.; Yang, K. R.; Regan, K. P.; Konezny, S. J.; Batista, V. S.; Brudvig, G. W.; Schmuttenmaer, C. A.; Kim, J. H. Facet-dependent photoelectrochemical performance of TiO2 nanostructures: an experimental and computational study. *J. Am. Chem. Soc.* **2015**, *137* (4), 1520−9.
(134) Wang, W. K.; Chen, J. J.; Lou, Z. Z.; Kim, S.; Fujitsuka, M.; Yu, H. Q.; Majima, T. Single-molecule and -particle probing crystal edge/corner as highly efficient photocatalytic sites on a single TiO2 particle. *Proc. Natl. Acad. Sci. USA* **2019**, *116* (38), 18827−18833.
(135) Zhan, W.; Alvarez, J.; Sun, L.; Crooks, R. M. A multichannel microfluidic sensor that detects anodic redox reactions indirectly using anodic electrogenerated chemiluminescence. *Anal. Chem.* **2003**, *75* (6), 1233−8.
(136) Saqib, M.; Lai, J. P.; Zhao, J. M.; Li, S. P.; Xu, G. B. Bipolar Electrochemical Approach with a Thin Layer of Supporting Electrolyte towards the Growth of Self-Organizing TiO2 Nanotubes. *ChemElectroChem* **2016**, *3* (3), 360−365.
(137) Chow, K. F.; Mavre, F.; Crooks, J. A.; Chang, B. Y.; Crooks, R. M. A large-scale, wireless electrochemical bipolar electrode microarray. *J. Am. Chem. Soc.* **2009**, *131* (24), 8364−5.
(138) Fosdick, S. E.; Crooks, R. M. Bipolar electrodes for rapid screening of electrocatalysts. *J. Am. Chem. Soc.* **2012**, *134* (2), 863−6.
(139) Al-Kutubi, H.; Voci, S.; Rassaei, L.; Sojic, N.; Mathwig, K. Enhanced annihilation electrochemiluminescence by nanofluidic confinement. *Chem. Sci.* **2018**, *9* (48), 8946−8950.
(140) Guo, W.; Zhou, P.; Sun, L.; Ding, H.; Su, B. Microtube Electrodes for Imaging the Electrochemiluminescence Layer and Deciphering the Reaction Mechanism. *Angew. Chem., Int. Ed.* **2021**, *60* (4), 2089−2093.
(141) Deiss, F.; LaFratta, C. N.; Symer, M.; Blicharz, T. M.; Sojic, N.; Walt, D. R. Multiplexed sandwich immunoassays using electrochemiluminescence imaging resolved at the single bead level. *J. Am. Chem. Soc.* **2009**, *131* (17), 6088−9.
(142) Dutta, P.; Han, D.; Goudeau, B.; Jiang, D.; Fang, D.; Sojic, N. Reactivity mapping of luminescence in space: Insights into heterogeneous electrochemiluminescence bioassays. *Biosens. Bioelectron.* **2020**, *165*, No. 112372.
(143) Sentic, M.; Milutinovic, M.; Kanoufi, F.; Manojlovic, D.; Arbault, S.; Sojic, N. Mapping electrogenerated chemiluminescence reactivity in space: mechanistic insight into model systems used in immunoassays. *Chem. Sci.* **2014**, *5* (6), 2568−2572.
(144) Fiorani, A.; Han, D.; Jiang, D.; Fang, D.; Paolucci, F.; Sojic, N.; Valenti, G. Spatially resolved electrochemiluminescence through a chemical lens. *Chem. Sci.* **2020**, *11* (38), 10496−10500.
(145) Han, D.; Fang, D.; Valenti, G.; Paolucci, F.; Kanoufi, F.; Jiang, D.; Sojic, N. Dynamic Mapping of Electrochemiluminescence Reactivity in Space: Application to Bead-Based Assays. *Anal. Chem.* **2023**, *95* (42), 15700−15706.
(146) Wu, Z.; Zeng, T.; Guo, W. J.; Bai, Y. Y.; Pang, D. W.; Zhang, Z. L. Digital Single Virus Immunoassay for Ultrasensitive Multiplex Avian Influenza Virus Detection Based on Fluorescent Magnetic Multifunctional Nanospheres. *ACS Appl. Mater. Interfaces* **2019**, *11* (6), 5762−5770.
(147) Zhang, F.; Shi, Q.; Zhang, Y.; Shi, Y.; Ding, K.; Zhao, D.; Stucky, G. D. Fluorescence upconversion microbarcodes for multiplexed biological detection: nucleic acid encoding. *Adv. Mater.* **2011**, *23* (33), 3775−9.
(148) Mahmood, A. Photovoltaic and Charge Transport Behavior of Diketopyrrolopyrrole Based Compounds with A−D−A−D−A Skeleton. *J. Clust. Sci.* **2019**, *30* (4), 1123−1130.
(149) Mahmood, A.; Abdullah, M. I.; Khan, S. U. Enhancement of nonlinear optical (NLO) properties of indigo through modification of

auxiliary donor, donor and acceptor. *Spectrochim. Acta A* **2015**, *139*, 425−30.
(150) Mahmood, A.; Khan, S. U.-D.; Rana, U. A. Theoretical designing of novel heterocyclic azo dyes for dye sensitized solar cells. *J. Comput. Electron.* **2014**, *13* (4), 1033−1041.
(151) Mahmood, A.; Tang, A.; Wang, X.; Zhou, E. First-principles theoretical designing of planar non-fullerene small molecular acceptors for organic solar cells: manipulation of noncovalent interactions. *Phys. Chem. Chem. Phys.* **2019**, *21* (4), 2128−2139.
(152) Mahmood, A.; Yang, J.; Hu, J.; Wang, X.; Tang, A.; Geng, Y.; Zeng, Q.; Zhou, E. Introducing Four 1,1-Dicyanomethylene-3-indanone End-Capped Groups as an Alternative Strategy for the Design of Small-Molecular Nonfullerene Acceptors. *J. Phys. Chem. C* **2018**, *122* (51), 29122−29128.
(153) Liu, J. L.; Zhang, J. Q.; Tang, Z. L.; Zhuo, Y.; Chai, Y. Q.; Yuan, R. Near-infrared aggregation-induced enhanced electrochemiluminescence from tetraphenylethylene nanocrystals: a new generation of ECL emitters. *Chem. Sci.* **2019**, *10* (16), 4497−4501.
(154) Long, X. Y.; Tan, X.; He, Y. P.; Zou, G. Z. Near-infrared electrochemiluminescence from non-toxic CuInS2 nanocrystals. *J. Mater. Chem. C* **2017**, *5* (47), 12393−12399.
(155) Ji, S. Y.; Zhao, W.; Gao, H.; Pan, J. B.; Xu, C. H.; Quan, Y. W.; Xu, J. J.; Chen, H. Y. Highly Efficient Aggregation-Induced Electrochemiluminescence of Polyfluorene Derivative Nanoparticles Containing Tetraphenylethylene. *iScience* **2020**, *23* (1), No. 100774.
(156) Carrara, S.; Aliprandi, A.; Hogan, C. F.; De Cola, L. Aggregation-Induced Electrochemiluminescence of Platinum(II) Complexes. *J. Am. Chem. Soc.* **2017**, *139* (41), 14605−14610.
(157) Liu, S.; Zhang, Q.; Zhang, L.; Gu, L.; Zou, G.; Bao, J.; Dai, Z. Electrochemiluminescence Tuned by Electron-Hole Recombination from Symmetry-Breaking in Wurtzite ZnSe. *J. Am. Chem. Soc.* **2016**, *138* (4), 1154−7.
(158) Wang, F.; Lin, J.; Zhao, T.; Hu, D.; Wu, T.; Liu, Y. Intrinsic "Vacancy Point Defect" Induced Electrochemiluminescence from Coreless Supertetrahedral Chalcogenide Nanocluster. *J. Am. Chem. Soc.* **2016**, *138* (24), 7718−24.
(159) Godeffroy, L.; Ciocci, P.; Ortiz Peña, N.; Alloyeau, D.; Noël, J.-M.; Lemineur, J.-F.; Kanoufi, F. Imaging the Footprint of Nanoscale Electrochemical Reactions for Assessing Synergistic Hydrogen Evolution. *Angew. Chem., Int. Ed.* **2023**, *62* (29), No. e202304950.
(160) Godeffroy, L.; Ciocci, P.; Nsabimana, A.; Miranda Vieira, M.; Noël, J.-M.; Combellas, C.; Lemineur, J.-F.; Kanoufi, F. Deciphering Competitive Routes for Nickel-Based Nanoparticle Electrodeposition by an Operando Optical Monitoring. *Angew. Chem., Int. Ed.* **2021**, *60* (31), 16980−16983.
(161) Godeffroy, L.; Lemineur, J.-F.; Shkirskiy, V.; Miranda Vieira, M.; Noël, J.-M.; Kanoufi, F. Bridging the Gap between Single Nanoparticle Imaging and Global Electrochemical Response by Correlative Microscopy Assisted By Machine Vision. *Small Methods* **2022**, *6* (9), No. 2200659.
(162) Godeffroy, L.; Makogon, A.; Gam Derouich, S.; Kanoufi, F.; Shkirskiy, V. Imaging and Quantifying the Chemical Communication between Single Particles in Metal Alloys. *Anal. Chem.* **2023**, *95* (26), 9999−10007.

https://doi.org/10.1021/acsmeasuresciau.3c00052
ACS Meas. Sci. Au 2024, 4, 3−24